

Complexation behavior of SrII and geochemically-related elements (MgII, CaII, BaII, and YIII) with biodegradable aminopolycarboxylate chelators (GLDA and HIDS)

メタデータ	言語: English 出版者: 公開日: 2018-02-15 キーワード (Ja): キーワード (En): 作成者: Begun, Zinnat A., Rahman, Ismail M.M., Hasegawa, Hiroshi, 長谷川, 浩 メールアドレス: 所属:
URL	https://doi.org/10.24517/00050117

This work is licensed under a Creative Commons Attribution 3.0 International License.



The research article is originally published at *Microchemical Journal*

An Elsevier Journal

<https://www.journals.elsevier.com/journal-of-molecular-liquids>

The original publication is available at: <https://doi.org/10.1016/j.molliq.2017.07.126>

Complexation Behavior of Sr^{II} and Geochemically-Related Elements (Mg^{II}, Ca^{II}, Ba^{II}, and Y^{III}) with Biodegradable Aminopolycarboxylate Chelators (GLDA and HIDS)

Zinnat A. Begum,^{1,2, †, *} Ismail M. M. Rahman,^{1, †, *} Hiroshi Hasegawa³

¹*Institute of Environmental Radioactivity, Fukushima University, 1 Kanayagawa, Fukushima City, Fukushima 960-1296, Japan*

²*Department of Civil Engineering, Southern University, 739/A Mehedibag Road, Chittagong 4000, Bangladesh*

³*Institute of Science and Engineering, Kanazawa University, Kakuma, Kanazawa 920-1192, Japan*

†Co-First Author

*Corresponding authors

E-mail: zinnat.ara@gmail.com or r801@ipc.fukushima-u.ac.jp (ZAB); i.m.m.rahman@gmail.com or immrahman@ipc.fukushima-u.ac.jp (IMMR)

Please Cite the article as: Z.A. Begum, I.M.M. Rahman and H. Hasegawa, Complexation behavior of Sr^{II} and geochemically-related elements (Mg^{II}, Ca^{II}, Ba^{II}, and Y^{III}) with biodegradable aminopolycarboxylate chelators (GLDA and HIDS), *Journal of Molecular Liquids*, 242: 1123-1130, 2017.

Abstract

The complexation of Sr^{II} and geochemically-related elements (Mg^{II}, Ca^{II}, Ba^{II}, and Y^{III}) with biodegradable aminopolycarboxylate chelators (DL-2-(2-carboxymethyl)nitriilotriacetic acid (GLDA) and 3-hydroxy-2,2'-iminodisuccinic acid (HIDS)) was evaluated with the objective of using in the chemical-induced washing remediation of radioactive solid waste. The stability constants ($\log_{10}K_{ML}$) for metal-chelator (ML) complexes between M (Mg^{II}, Ca^{II}, Sr^{II}, Ba^{II}, or Y^{III}) and L (GLDA or HIDS) in the aqueous matrix was derived from experimental potentiometric data (M:L = 1:1; ionic strength, $I = 0.10 \text{ mol}\cdot\text{dm}^{-3}$; $T = 25 \pm 0.1^\circ\text{C}$). The formation of ML^{2-} species was dominant in the systems with Mg^{II}, Ca^{II}, Sr^{II}, or Ba^{II}, while $M(OH)L^{2-}$ or $M(OH)_2L^{3-}$ was the major species with Y^{III}. The stability of Y^{III}-L complexes was higher than that of Mg^{II}, Ca^{II}, Sr^{II}, or Ba^{II}, while the order for complexation strength of GLDA and HIDS was not similar with divalent ions: M-GLDA ($\log_{10}K_{Mg-L} < \log_{10}K_{Ca-L} > \log_{10}K_{Sr-L} > \log_{10}K_{Ba-L}$), M-HIDS ($\log_{10}K_{Mg-L} > \log_{10}K_{Ca-L} > \log_{10}K_{Sr-L} > \log_{10}K_{Ba-L}$). The conditional stability constants for the ML systems was also derived in terms of pH (2 to 12), and compared with that of EDTA and EDDS. The data trend indicated that the overall stability of the complexes of Mg^{II}, Ca^{II}, Sr^{II}, Ba^{II}, or Y^{III} with GLDA or HIDS was better than the biodegradable chelator EDDS, which was frequently recommended as the alternative to EDTA.

Keywords

Stability constant; biodegradable chelating agents; GLDA; HIDS; Strontium; Yttrium

1.0 Introduction

Radiostrontium (r-Sr) enters in the ecosystem on a global scale from the above-ground nuclear weapon tests, and on a local level due to the accidental release or improper waste disposal from nuclear technology-related activities [1]. The ^{90}Sr , which is the longest-lived r-Sr isotope produced from nuclear fission (^{90}Sr , $t_{1/2} = 28.9$ years; ^{89}Sr , $t_{1/2} = 50.6$ days; ^{85}Sr , $t_{1/2} = 64.85$ days), evoke ecological concern [2] because of the high mobility characteristics compared to many other radionuclides [3]. A greater fraction of residual r-Sr in soil remains in the upper 10 cm layer despite a migration velocity of 0.7–1.5 cm year⁻¹ [4, 5]. Therefore, the accumulation of r-Sr in soils can affect the human health through the food chain [6, 7].

The major options to treat the r-Sr contaminated solids are natural attenuation and artificial decontamination [8, 9]. The techniques adopted for soil remediation include solidification/stabilization, soil flushing, phytoremediation, and so forth [10, 11], while ex-situ washing received significant attention for their wide applicability and economic feasibility [12-14]. Washing remediation incorporates either or both physical and chemical processes to confine the contaminants in soils [14, 15]. Aminopolycarboxylate chelators (APCs), which capable of creating stable complexes with elements, are commonly recommended as the additive to the washing solution used for contaminated soil treatment [16-18]. The classical APCs, such as EDTA (ethylenediaminetetraacetic acid), DTPA (diethylenetriaminepentaacetic acid), or their homologs, however, persist in the environment because of poor photo-, chem-, and biodegradability resulting lethal exposures [19-22]. Several eco-friendly biodegradable alternatives to classical APCs, e.g., IDSA (iminodisuccinic acid), EDDS (ethylenediamine-*N,N'*-disuccinic acid), MGDA (methylglycinediacetic acid) has, thus, been proposed, while application of EDDS was extensively focused in the literature [23-26].

Although the corresponding metal-chelator stability induces partial selectivity toward ions in a matrix during chelator-assisted soil remediation, a higher metal to chelator ratio has been recommended to minimize the competing impacts of the coexisting geochemically similar ions [13]. Sr^{II} , being a lithophile element, is mainly associated with calcium (Ca^{II}) and with magnesium (Mg^{II}) to a smaller extent. Ca^{II} , which contributes more than 90% of the total cation content in many soils, have a fairly similar ionic radius to that of Sr^{II} and possess similar geochemical and biochemical features [27]. The ionic radius of Sr^{II} is analogous to barium

(Ba^{II}) and also has geochemical similarity [28]. Besides, the ⁹⁰Sr undergoes β^- decay into yttrium-90 (⁹⁰Y; $t_{1/2} = 64.1$ h), and it remains in secular equilibrium in the environment with its parent isotope, ⁹⁰Sr [2]. The biogeochemical behavior of stable Sr-isotopes (⁸⁴Sr, ⁸⁶Sr, or ⁸⁸Sr) similar to that of ⁹⁰Sr [29], and therefore, used as a natural analog to r-Sr in the current work. Our research group previously reported the effect of operating variables on the application of DL-2-(2-carboxymethyl)nitrilotriacetic acid (GLDA) and 3-hydroxy-2,2'-iminodisuccinic acid (HIDS) for the washing remediation of soils [30, 31]. Both GLDA [32] and HIDS [33] claimed to possess superior biodegradable characteristics relative to EDTA, DTPA or its homologs. The formation and stability of ML (M, metal; L, chelator) species at different equilibrium conditions in the environment affect metal-bioavailability and corresponding physiological or toxicological behavior [34]. Hence, the protonation and complexation behavior of GLDA and HIDS with several ecologically important ions (Ni^{II}, Cu^{II}, Zn^{II}, Cd^{II}, Pb^{II}, Fe^{III}, and Cr^{III}; ionic strength, $I = 0.1$ or $1.0 \text{ mol}\cdot\text{dm}^{-3}$; $T = 25 \text{ }^\circ\text{C}$) in the aqueous matrix was focused in our previous reports [35, 36].

The objective of present work is to evaluate the complexation behavior of Sr^{II} and its geochemically related elements (Ba^{II}, Ca^{II}, Mg^{II}, and Y^{III}) with GLDA and HIDS. The data has not been reported before in the standard reference databases, and can be useful in chemical-enhanced washing remediation of strontium-laden hazardous wastes, such as residuals from nuclear energy-related facilities.

2.0 Experimental

2.1 Materials

The biodegradable aminopolycarboxylate chelators, GLDA (AkzoNobel; Amsterdam, Netherlands; 40 wt%) and HIDS (Nippon Shukubai; Tokyo, Japan; 50 wt%) (Table 1), were obtained as the aqueous solution of corresponding tetra-sodium salt and used without further treatment. Analytical grade reagents, all procured from Kanto Chemical (Tokyo, Japan) unless mentioned otherwise, were used without any additional purification. Potassium hydroxide (KOH, CO₂-free) and nitric acid (HNO₃) were used for the potentiometric titration, and potassium nitrate (KNO₃) was used as the background electrolyte for maintaining the solution

ionic strength. Potassium hydrogen phthalate was utilized for the standardization of KOH. The standard pH solutions (Horiba 101-S; Kyoto, Japan) were used for glass electrode calibration. Aqueous solutions of Mg^{II} , Ca^{II} , Sr^{II} , Ba^{II} , and Y^{III} were prepared, respectively, from calcium nitrate tetrahydrate, magnesium nitrate hexahydrate, barium nitrate, strontium nitrate (Kanto Chemical; Tokyo, Japan) and yttrium chloride anhydrous (Sigma-Aldrich; St. Louis, MO, USA). Single element standard solutions ($1000 \text{ mg}\cdot\text{dm}^{-3}$) of Ca, Mg, Sr and Y from SpecCertiPrep (Metuchen, NJ, USA) and Ba from Kanto Chemical (Tokyo, Japan) were used for mass-spectrophotometric determination. All the working solutions were prepared by dilution of the stock reagents with ultrapure water (resistance $>18 \text{ m}\Omega\cdot\text{cm}$, total organic content $<1 \mu\text{g}\cdot\text{dm}^{-3}$) from a PureLab Ultra Analytic system (ELGA Lab Water; Celle, Germany).

2.2 Methods

2.2.1 Potentiometric measurements

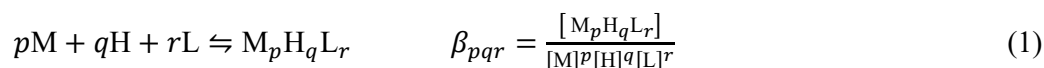
The formation constants of ML complexes was estimated from potentiometric measurements data obtained using the KEM AT-710 automatic titrator (Kyoto Electronics; Kyoto, Japan), equipped with a pH-combination electrode and a temperature probe. The titration assembly included a magnetic stirrer and a sealed 100 cm^3 titration vessel with inlets for the electrode, temperature probe and dosing nozzle from the titrator, in addition to inlet and outlet for N_2 gas. The KOH ($0.1 \text{ mol}\cdot\text{dm}^{-3}$) was the titrant, while the titers contained HNO_3 ($1.0 \times 10^{-2} \text{ mol}\cdot\text{dm}^{-3}$), L (GLDA or HIDS; $1.0 \times 10^{-3} \text{ mol}\cdot\text{dm}^{-3}$) and M (Mg^{II} , Ca^{II} , Sr^{II} , Ba^{II} , or Y^{III} ; $1.0 \times 10^{-3} \text{ mol}\cdot\text{dm}^{-3}$). The titer also spiked with an appropriate volume of $1.0 \text{ mol}\cdot\text{dm}^{-3} \text{ KNO}_3$ to maintain $I = 0.1 \text{ mol}\cdot\text{dm}^{-3}$. The total volume of each mixture was maintained at 50 cm^3 . The solution temperature was maintained at $25 \pm 0.1^\circ\text{C}$ using a control system combined with a jacketed heat exchanger bath (SKG-01, AS ONE; Tokyo, Japan), a constant temperature water heater (TBK202HA, Advantec; Tokyo, Japan) and a thermo-controlled water circulator (Eyela CTP-1000, Tokyo Rikakikai; Tokyo, Japan). The inert conditions within the solution system were achieved by a continuous flow of N_2 gas, which also eliminated the ingress of CO_2 . The electrode system was calibrated at pH 4.0, 7.0 and 9.0 after each potentiometric measurement using standard pH solutions. The metal concentration in the working mixtures was confirmed using the Nexion 350S inductively coupled plasma mass spectrometer (Perkin Elmer; Shelton,

CT, USA), while the GLDA and HIDS concentrations were validated using an automated high-performance liquid chromatography system (TOSOH 8020, TOSOH; Tokyo, Japan).

2.2.2 Processing of the experimental potentiometric data

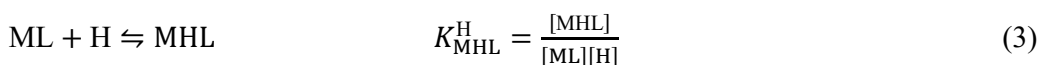
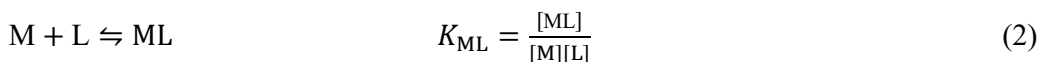
2.2.2.1 Equations

The overall complex formation constants ($\log_{10}\beta_{pqr}$) of each ML system were determined from the composition model considering the consistency with the potentiometric titration data, logical appropriateness of the chemical approach and better statistical fitting than the other alternatives. The following equation was used to describe the overall stoichiometry associated with the possible equilibria in solution for ML systems:

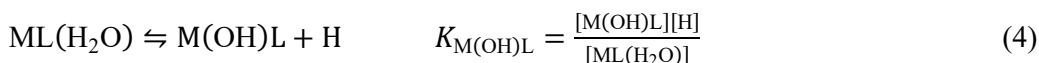


In Eq (1), the stoichiometric coefficients for metal ion, proton, and chelator in an ML system during the possible equilibria in solution were represented using following respective symbols: p , q , and r .

The following equations were used to define the stepwise formation constant ($\log_{10}K$) in the ML systems:



The following equation was used to define the coordination of water molecules, which involves additional deprotonation reactions in the ML systems:



The $\log_{10}\beta_{pqr}$ provides crucial stability information of an ML species [37], while it does not consider the impacts of changes in system equilibrium conditions due to pH or interference from coexistent species. Hence, the term ‘conditional stability constant ($\log_{10}K'_{ML}$)’ was introduced and defined using the following equation:

$$\log_{10}K'_{ML} \rightleftharpoons \log_{10}K_{ML} - \log\alpha_{HL} - \log\alpha_M + \log\alpha_{ML} \quad (5)$$

In Eq (5), $\log_{10}K_{ML}$ denoted the formation constant of ML complexes at a 1:1 molar ratio. The $\log_{10}\alpha_{HL}$, $\log_{10}\alpha_M$, and $\log_{10}\alpha_{ML}$ were used, respectively, to express the effect of side reactions for the protonation of chelator, metal hydroxides formation, and MHL (metal-proton-chelator species) or M(OH)L (metal-hydroxo-chelator species) formation.

2.2.2.2 Computation software

An analysis of strong acid-strong base titration results by GLEE [38] provided the estimation of carbonate contamination, electrode potential (E^0), and slope factor (S) (hydrolysis constant of water, $pK_w = 13.79$, $I = 0.1 \text{ mol}\cdot\text{dm}^{-3}$ at $25 \pm 0.1^\circ\text{C}$, supporting electrolyte: KNO_3). The HySS2009 [39] was used to simulate the titration conditions before the real experiments. The formation and stability constants of the ML complexes were computed using the experimental potentiometric data (see supplementary information file: Table S1–S3) and the protonation constants for GLDA or HIDS ($I = 0.1 \text{ mol}\cdot\text{dm}^{-3}$; $T = 25 \pm 0.1^\circ\text{C}$) [36] using HYPERQUAD 2008 [40].

3.0 Results and discussion

3.1 Stability characteristics of metal-chelator complexes

3.1.1 M^{II} -L

The $\log_{10}\beta_{pqr}$ for the ML systems containing M (Mg^{II} , Ca^{II} , Sr^{II} , or Ba^{II}) and L (GLDA or HIDS) were computed from the experimental potentiometric data (Tables 2 and 3). The complexation between metal and APCs was characterized by the formation of stable mononuclear 1:1 metal to chelator complexes because the ML species dominantly occurred in all the systems (Table 5). The $\log_{10}K$ for each of the species in ML systems was calculated from the differences of $\log_{10}\beta$ values and compared with those of EDDS and EDTA (Table 6).

The formation of ML complexes started in the acid region ($\text{pH} \sim 5$) ($M = \text{Mg}^{II}$, Ca^{II} , Sr^{II} , or Ba^{II} ; $L = \text{GLDA}$ or HIDS) as evident from the titration curves (Figure 1), indicating the dissociation of two protons from chelators before the complexation initiated with metals. The $\log_{10}K_{ML}$ values obtained for Mg^{II} , Sr^{II} , or Ba^{II} -HIDS complexes were found to be greater than the corresponding values for M-GLDA complexes, while the magnitude was opposite for Ca^{II} -L ($L = \text{GLDA}$ or HIDS) complexes. The formation of stable metal-hydroxo complexes

($M(OH)L^{3-}$; $M = Mg^{II}$, Sr^{II} , or Ba^{II} ; $L = GLDA$ or $HIDS$) were started for $GLDA$ containing ML systems at $pH \sim 9$, and for $HIDS$ at $pH \sim 8$. The $M(OH)L^{3-}$ complex did not occur in the $Ca^{II} + GLDA$ system, while $Ca(OH)HIDS^{3-}$ appeared at $pH \sim 8$.

The species distribution curves for the $M-GLDA$ or $M-HIDS$ system ($M = Mg^{II}$, Ca^{II} , Sr^{II} , or Ba^{II} ; $L = GLDA$ or $HIDS$) showed that the ML complexes were formed in increasing proportions beginning at $pH 5$ (Figure 3). The highest formation was observed at $pH > 9$ ($Mg^{II}-GLDA$, 92%, $pH 9.6$; $Mg^{II}-HIDS$, 82%, $pH 9.2$; $Ca^{II}-HIDS$, 89%, $pH 9.5$; $Sr^{II}-GLDA$, 70%, $pH 10$; $Sr^{II}-HIDS$, 64%, $pH 9.2$; $Ba^{II}-GLDA$, 60%, $pH 9.8$; $Ba^{II}-HIDS$, 46%, $pH 9.6$), with the exception for $Ca^{II}-GLDA$ at 90 to 98% from $pH 8.1$ to higher for the total metals present at $pH 5$ to 12. The species $Ca(OH)GLDA^{3-}$ was not occurred in the system, while $M(OH)L^{3-}$ was observed with other ions ($M = Mg^{II}$, Sr^{II} , or Ba^{II} , $L = GLDA$; or $M = Mg^{II}$, Ca^{II} , Sr^{II} , or Ba^{II} , $L = HIDS$). The $\log_{10}K_{ML}$ for $M-HIDS$ was higher than that of the $M-GLDA$, while the formation rate showed the inverse ($M = Mg^{II}$, Sr^{II} , or Ba^{II}) followed by a greater formation ratio of $M(OH)HIDS^{3-}$. The tendency indicated that the $\log_{10}K_{ML}$ value for an ML system accounts not only the formation rate of ML species within the system but also depends on the formation rate of other species, e.g., MHL , $M(OH)L$.

The stability constant data ($\log_{10}K_{ML}$) obtained for the complexation of Mg^{II} , Ca^{II} , Sr^{II} , or Ba^{II} and $GLDA$ are comparable to the data in the 'NIST Critically Selected Stability Constants of Metal Complexes Database' [41] (see the parenthesis in Table 6). However, the reference database does not include any data for the metal-hydroxo complexes of $GLDA$ with Mg^{II} , Sr^{II} , or Ba^{II} , and no data is also available for $M-HIDS$ systems in the same database.

3.1.2 $M^{III}-L$

The species distribution curves (Figure 4) in the range of $pH 2$ to 12 ($I = 0.1 \text{ mol}\cdot\text{dm}^{-3}$) confirmed the formation of MHL complexes ($M = Y^{III}$; $L = GLDA$ or $HIDS$) from $pH \sim 2$. The MHL was expected to form by the coordination of weakly basic imine nitrogen atom and the deprotonated carboxylic group in $GLDA$ or $HIDS$. The water molecules attached with the metals were supposed to be replaced with the increase of pH facilitating the deprotonation of carboxylic groups in $GLDA$ or $HIDS$, and leads to the formation of the ML^{-} , $M(OH)L^{2-}$ and $M(OH)_2L^{3-}$ complexes. The formation of $M(OH)_3L^{4-}$ species was also observed in the $Y^{III}-HIDS$ system (Table 4).

The titration curves for the Y^{III} -L systems (L = GLDA or HIDS; $I = 0.1 \text{ mol}\cdot\text{dm}^{-3}$; $T = 25 \pm 0.1^\circ\text{C}$) showed a second inflection at higher pH values (Figure 2), which indicated the formation of hydrolyzed ML complexes [42]. The dominant species in the Y^{III} -L systems were metal-hydroxo species with the highest formation ratio of $Y(\text{OH})\text{GLDA}^{2-}$ (98%) at pH 7.3 to 8.9, $Y(\text{OH})\text{HIDS}^{2-}$ (94%) at pH 5.1, and $Y(\text{OH})_2\text{HIDS}^{3-}$ (96%) at pH 8.4 (Table 5).

The $\log_{10}K_{ML}$ data for complexation between GLDA or HIDS and Y^{III} ($I = 0.1 \text{ mol}\cdot\text{dm}^{-3}$; $25 \pm 0.1^\circ\text{C}$) (Table 6) was not available in the reference database [41] for comparison with the current results.

3.2 Trends in complexation behavior

3.2.1 M^{II} -L

The atomic radius (calculated in picometers) [43, 44] of the elements considered in the present study has the following order: Mg^{II} (145) < Ca^{II} (194) < Sr^{II} (219) < Ba^{II} (253). The stabilities of ML complexes ($\log_{10}K_{ML}$) decreased with increasing atomic radius of ions as observed for M-HIDS complexes: $\log_{10}K_{MgL} > \log_{10}K_{CaL} > \log_{10}K_{SrL} > \log_{10}K_{BaL}$ (5.57 > 5.05 > 4.7 > 3.8) (Table 3). However, the stability order of complexes with GLDA were as follows: $\log_{10}K_{MgL} < \log_{10}K_{CaL} > \log_{10}K_{SrL} > \log_{10}K_{BaL}$ (5.31 < 5.88 > 4.04 > 3.64) (Table 2). The ‘irregular’ position of Mg^{II} in the series [45] can be attributable to the weaker coordination of smaller Mg^{II} ion with GLDA [46], or better fit of Ca^{II} than the Mg^{II} within the stereo-configuration of M-GLDA [47, 48].

The $\log_{10}K_{ML}$ values of GLDA or HIDS complexes with Mg^{II} , Ca^{II} , Sr^{II} , or Ba^{II} was compared with the corresponding $\log_{10}K_{ML}$ values of some divalent ecotoxic ions (Ni^{II} , Cu^{II} , Zn^{II} , Cd^{II} , or Pb^{II}), as reported in the literature [36], to evaluate the extended trend (Figure 5). The $\log_{10}K_{M-GLDA}$ were in the higher order with Ni^{II} , Cu^{II} , Zn^{II} , Cd^{II} , or Pb^{II} than the corresponding $\log_{10}K_{M-HIDS}$. A similar trend was observed for the ML complexes with Ca^{II} , while it was opposite ($\log_{10}K_{M-HIDS} > \log_{10}K_{M-GLDA}$) for Mg^{II} , Sr^{II} , or Ba^{II} .

3.2.2 M^{III} -L

The $\log_{10}K_{ML}$ for Y^{III} -L complexes were much higher than that observed for divalent Mg^{II} , Ca^{II} , Sr^{II} , or Ba^{II} . The $\log_{10}K_{Y-GLDA}$ (14.75) was greater than the $\log_{10}K_{Y-HIDS}$ (12.75), and the trend ($\log_{10}K_{M-GLDA} > \log_{10}K_{M-HIDS}$) was similar to that reported for Fe^{III} -L or Cr^{III} -L complexes (L

= GLDA or HIDS) [35]. The comparison of $\log_{10}K_{ML}$ values (Figure 6) confirmed a similar order ($\log_{10}K_{Cr-L} < \log_{10}K_{Fe-L} < \log_{10}K_{Y-L}$) with both chelators, which followed the pattern of corresponding atomic radius (calculated in picometers) [43, 44] of the elements: Cr^{III} (140) < Fe^{III} (156) < Y^{III} (212).

3.3 Conditional stability constant of metal-chelator complexes

3.3.1 M^{II} -L

The stability of an ML complex depends on the type of interaction (e.g., electrostatic or covalent) between metal and chelator, which is determined by several factors, such as coordination and oxidation behavior of the metal and chemical structure of the chelator [49]. The effects of side reactions during metal-chelator complexation can be explained using the $\log_{10}K'_{ML}$ values [50].

The $\log_{10}K'_{ML}$ for ML complexes ($M = Mg^{II}$, Ca^{II} , Sr^{II} , or Ba^{II} ; $L = GLDA$ or $HIDS$; $I = 0.1 \text{ mol}\cdot\text{dm}^{-3}$; $T = 25 \pm 0.1 \text{ }^{\circ}\text{C}$) has been computed in the pH range of 2 to 12 using HySS2009 program [39] based on the corresponding experimental $\log_{10}K_{ML}$ values, and illustrated in Figure 7. The $\log_{10}K'_{ML}$ values for M-GLDA or M-HIDS was further compared with that of EDTA and EDDS. The order of $\log_{10}K'_{ML}$ for M-HIDS complexes varied in a reciprocal order to the corresponding atomic radius of the elements, i.e., $Mg^{II} > Ca^{II} > Sr^{II} > Ba^{II}$, and was similar to the pattern observed for M-EDDS systems. The order of $\log_{10}K'_{ML}$ for M-GLDA ($Mg^{II} < Ca^{II} > Sr^{II} > Ba^{II}$) was similar to that of M-EDTA. The $\log_{10}K'_{ML}$ trend indicated that the EDTA complexes with Mg^{II} , Ca^{II} , Sr^{II} , or Ba^{II} displayed better stability than the ML systems containing biodegradable chelators (GLDA, HIDS, or EDDS) irrespective of the solution pH. The $\log_{10}K'_{ML}$ values also indicated the limited applicability of GLDA, HIDS or EDDS below pH 7. The order of $\log_{10}K'_{ML}$ ($M = Mg^{II}$, Ca^{II} , Sr^{II} , or Ba^{II}) at pH 7 or above have followed either of the following patterns: $\log_{10}K'_{M-EDTA} > \log_{10}K'_{M-HIDS} > \log_{10}K'_{M-GLDA} > \log_{10}K'_{M-EDDS}$, or $\log_{10}K'_{M-EDTA} > \log_{10}K'_{M-GLDA} > \log_{10}K'_{M-HIDS} > \log_{10}K'_{M-EDDS}$. The trend confirmed a superior stability of M-GLDA or M-HIDS complexes than the corresponding M-EDDS ($M = Ca^{II}$, Sr^{II} , or Ba^{II}), while the difference became insignificant for Mg^{II} -L ($L = GLDA$, $HIDS$ or $EDDS$) above pH 7.

3.3.2 M^{III} -L

The complexation between Y^{III} and EDTA was marginally stronger than that of GLDA or HIDS in the acidic pH (pH 4: $\log_{10}K'_{Y-EDTA} > \log_{10}K'_{Y-GLDA} > \log_{10}K'_{Y-HIDS} > \log_{10}K'_{Y-EDDS}$), while the Y^{III} -GLDA has better stability than the other Y^{III} -L systems in the neutral pH (pH 7: $\log_{10}K'_{Y-GLDA} > \log_{10}K'_{Y-EDTA} > \log_{10}K'_{Y-HIDS} > \log_{10}K'_{Y-EDDS}$). The stability order of Y^{III} -L complexes at pH ≥ 8 ($\log_{10}K'_{Y-HIDS} > \log_{10}K'_{Y-GLDA} > \log_{10}K'_{Y-EDTA} > \log_{10}K'_{Y-EDDS}$) indicated a better complexation capability of HIDS compared to the GLDA with Y^{III} , and both the biodegradable chelators performed better than the EDTA. The stability of Y^{III} complexes with GLDA or HIDS was significantly higher than the corresponding complexes with EDDS irrespective of the pH in the range of 2 to 12 (Figure 8).

The $\log_{10}K'_{ML}$ patterns of Y^{III} -L complexes in acidic, neutral or basic pH conditions have not been consistent with the sequence of overall stability constant values ($\log_{10}K_{Y-EDTA} > \log_{10}K_{Y-GLDA} > \log_{10}K_{Y-EDDS} > \log_{10}K_{Y-HIDS}$) (Table 6). The inconsistency might be attributable to the lack of hydrolyzed species formation within the ML systems, as stated in the standard literature sources [41] for the EDDS or EDTA.

4.0 Conclusion

The complexation characteristics of Mg^{II} , Ca^{II} , Sr^{II} , Ba^{II} , or Y^{III} (M) with GLDA or HIDS (L), both established to be biodegradable in the environment, was calculated using experimental potentiometric data. The $\log_{10}K_{M-GLDA}$ was higher than $\log_{10}K_{M-HIDS}$ for Ca^{II} -L or Y^{III} -L systems, while an opposite trend was observed for the ML systems of Mg^{II} , Sr^{II} , or Ba^{II} . The conditional stability of ML complexes in the aqueous matrix in terms of pH (2–12) indicated a stronger complexation tendency in the basic pH conditions, and a narrower working pH range effective from neutral region. The complexation aptitude of GLDA or HIDS was lower than the EDTA with Mg^{II} , Ca^{II} , Sr^{II} , or Ba^{II} irrespective of the solution pH, and with Y^{III} in the acidic pH. However, the GLDA or HIDS has the advantage of lower post-operation ecotoxicity and is recommended to include in consideration as an alternative to EDTA. Moreover, the GLDA or HIDS is also recommended as the superior biodegradable alternative relative to EDDS for the chelator-assisted washing remediation of solid waste containing Mg^{II} , Ca^{II} , Sr^{II} , Ba^{II} , or Y^{III} , while HIDS is the better substitute than the GLDA.

Acknowledgement

This research was partially supported by the funds from (a) Grants-in-Aid for Scientific Research (17K00622) from the Japan Society for the Promotion of Science (JSPS), (b) Science and Technology Research Partnership for Sustainable Development (SATREPS), Japan Science and Technology Agency (JST)/Japan International Cooperation Agency (JICA), and (c) Interdisciplinary Project on Environmental Transfer of Radionuclides (FY2016, F-1-A; FY2017, F-5-A) collaborated with Center for Research in Isotopes and Environmental Dynamics (CRiED), University of Tsukuba, Japan.

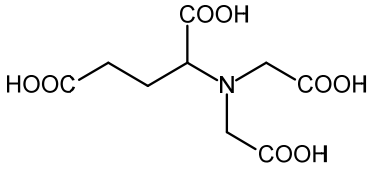
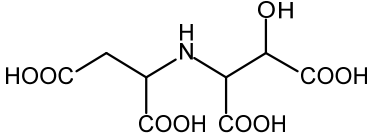
References

- [1] C.F.V. Mason, N. Lu, J. Conca, in: S.S. Hecker, C.F.V. Mason, K.K. Kadyrzhanov, S.B. Kislitsin (Eds.), *Nuclear Physical Methods in Radioecological Investigations of Nuclear Test Sites*, Springer Netherlands, Dordrecht, 2000, p. 89-97.
- [2] N. Vajda, C.-K. Kim, *Appl. Radiat. Isot.* 68 (2010) 2306-2326.
- [3] L.M. Kagan, V.B. Kadatsky, *J. Environ. Radioact.* 33 (1996) 27-39.
- [4] G. Arapis, E. Petrayev, E. Shagalova, O. Zhukova, G. Sokolik, T. Ivanova, *J. Environ. Radioact.* 34 (1997) 171-185.
- [5] E. Shagalova, O. Zhukova, M. Germenchuk, I. Matveencko, Z. Bakarikova, *J. Radioanal. Nucl. Chem.* 246 (2000) 521-525.
- [6] P.N. Chiang, M.K. Wang, P.M. Huang, J.J. Wang, C.Y. Chiu, *J. Environ. Radioact.* 101 (2010) 472-481.
- [7] A. Rigol, M. Roig, M. Vidal, G. Rauret, *Environ. Sci. Technol.* 33 (1999) 887-895.
- [8] IAEA, International Atomic Energy Agency, Vienna, Austria, 2006, p. 105.
- [9] K. Maslova, I. Stepina, A. Konoplev, V. Popov, A. Gusarov, F. Pankratov, S.D. Lee, N. Il'icheva, *J. Environ. Radioact.* 125 (2013) 74-80.
- [10] G. Dermont, M. Bergeron, G. Mercier, M. Richer-Lafleche, *Pract. Period. Hazard. Toxic Radioact. Waste Manage.* 12 (2008) 188-209.
- [11] I.M.M. Rahman, Z.A. Begum, H. Sawai, in: H. Hasegawa, I.M.M. Rahman, M.A. Rahman (Eds.), *Environmental Remediation Technologies for Metal-Contaminated Soils*, Springer, Tokyo, Japan, 2016, p. 125-146.
- [12] Z.A. Begum, I.M.M. Rahman, H. Sawai, H. Hasegawa, in: H. Hasegawa, I.M.M. Rahman, M.A. Rahman (Eds.), *Environmental Remediation Technologies for Metal-Contaminated Soils*, Springer, Tokyo, Japan, 2016, p. 197-218.
- [13] A. Ferraro, M. Fabbicino, E.D. van Hullebusch, G. Esposito, F. Pirozzi, *Rev. Environ. Sci. Biotechnol.* 15 (2016) 111-145.
- [14] G. Dermont, M. Bergeron, G. Mercier, M. Richer-Lafleche, *J. Hazard. Mater.* 152 (2008) 1-31.
- [15] P. Robert W, *J. Hazard. Mater.* 66 (1999) 151-210.
- [16] D. Leštan, C.L. Luo, X.D. Li, *Environ. Pollut.* 153 (2008) 3-13.
- [17] H. Hasegawa, I.M.M. Rahman, S. Kinoshita, T. Maki, Y. Furusho, *Chemosphere* 79 (2010) 193-198.

- [18] H. Hasegawa, I.M.M. Rahman, M. Nakano, Z.A. Begum, Y. Egawa, T. Maki, Y. Furusho, S. Mizutani, *Water Res.* 45 (2011) 4844–4854.
- [19] I.M.M. Rahman, M.M. Hossain, Z.A. Begum, M.A. Rahman, H. Hasegawa, in: I.A. Golubev (Ed.) *Handbook of Phytoremediation*, Nova Science Publishers, New York, 2010, p. 709–722.
- [20] B. Nowack, *Environ. Sci. Technol.* 36 (2002) 4009–4016.
- [21] T. Egli, *J. Biosci. Bioeng.* 92 (2001) 89–97.
- [22] M. Sillanpää, A. Oikari, *Chemosphere* 32 (1996) 1485–1497.
- [23] S. Tandy, K. Bossart, R. Mueller, J. Ritschel, L. Hauser, R. Schulin, B. Nowack, *Environ. Sci. Technol.* 38 (2004) 937–944.
- [24] J. Pichtel, T.M. Pichtel, *Environ. Eng. Sci.* 14 (1997) 97–104.
- [25] L. Zhang, Z. Zhu, R. Zhang, C. Zheng, H. Zhang, Y. Qiu, J. Zhao, *J. Environ. Sci.* 20 (2008) 970–974.
- [26] L. Hauser, S. Tandy, R. Schulin, B. Nowack, *Environ. Sci. Technol.* 39 (2005) 6819–6824.
- [27] A. Kabata-Pendias, *Trace Elements in Soils and Plants* (4th Edition). 4th edn. CRC press, Boca Raton, FL, 2010.
- [28] A. Jeske, *Soil Science Annual*, 2013, p. 2-7.
- [29] H. Tsukada, A. Takeda, T. Takahashi, H. Hasegawa, S.i. Hisamatsu, J. Inaba, *J. Environ. Radioact.* 81 (2005) 221-231.
- [30] Z.A. Begum, I.M.M. Rahman, H. Sawai, S. Mizutani, T. Maki, H. Hasegawa, *Water Air Soil Pollut.* 224 (2013) 1381.
- [31] Z.A. Begum, I.M.M. Rahman, Y. Tate, H. Sawai, T. Maki, H. Hasegawa, *Chemosphere* 87 (2012) 1161–1170.
- [32] *Dissolvine® GL Technical Brochure*, Akzo Nobel Amsterdam, The Netherlands, 2004.
- [33] *Biodegradable Chelating Agent: HIDS*, Nippon Shokubai, Osaka, Japan, 2008.
- [34] A.E. Angkawijaya, A.E. Fazary, E. Hernowo, M. Taha, Y.-H. Ju, *J. Chem. Eng. Data* 56 (2011) 532-540.
- [35] Z.A. Begum, I.M.M. Rahman, H. Sawai, Y. Tate, T. Maki, H. Hasegawa, *J. Chem. Eng. Data* 57 (2012) 2723–2732.
- [36] Z.A. Begum, I.M.M. Rahman, Y. Tate, Y. Egawa, T. Maki, H. Hasegawa, *J. Solution Chem.* 41 (2012) 1713–1728.

- [37] A.E. Martell, R.D. Hancock, *Metal Complexes in Aqueous Solutions*. Plenum Press, New York, 1996.
- [38] P. Gans, B. O'Sullivan, *Talanta* 51 (2000) 33–37.
- [39] L. Alderighi, P. Gans, A. Ienco, D. Peters, A. Sabatini, A. Vacca, *Coordin. Chem. Rev.* 184 (1999) 311–318.
- [40] P. Gans, A. Sabatini, A. Vacca, *Talanta* 43 (1996) 1739–1753.
- [41] A.E. Martell, R.M. Smith, R.J. Motekaitis, Texas A&M University, College Station, TX, 2004.
- [42] S.S. Jones, F.A. Long, *J. Phys. Chem.* 56 (1952) 25-33.
- [43] E. Clementi, D.L. Raimondi, *J. Chem. Phys.* 38 (1963) 2686-2689.
- [44] E. Clementi, D.L. Raimondi, W.P. Reinhardt, *J. Chem. Phys.* 47 (1967) 1300-1307.
- [45] R.K. Cannan, A. Kibrick, *J. Am. Chem. Soc.* 60 (1938) 2314-2320.
- [46] E.T. Clarke, A.E. Martell, *Inorg. Chim. Acta* 190 (1991) 27-36.
- [47] R. Aruga, *Inorg. Chem.* 19 (1980) 2895-2896.
- [48] R.J. Motekaitis, A.E. Martell, *Inorg. Chem.* 28 (1989) 3499-3503.
- [49] C.F. Bell, *Principles and Applications of Metal Chelation*. Clarendon Press, Oxford, 1977.
- [50] J. Davidge, C.P. Thomas, D.R. Williams, *Chem. Speciation Bioavailability* 13 (2001) 129–134.

Table 1: Chemical Structure and the Overall Protonation Constants ($\log_{10}\beta_{pqr}$) of the Biodegradable Aminopolycarboxylate Chelators ^{a, b}

Chelator	Chemical structure	Protonation equilibria	$\log_{10}\beta_{pqr}$
GLDA		$\text{GLDA}^{4-} + \text{H}^+ \rightleftharpoons \text{HGLDA}^{3-}$	9.39
		$\text{HGLDA}^{3-} + \text{H}^+ \rightleftharpoons \text{H}_2\text{GLDA}^{2-}$	14.40
		$\text{H}_2\text{GLDA}^{2-} + \text{H}^+ \rightleftharpoons \text{H}_3\text{GLDA}^{-}$	17.89
		$\text{H}_3\text{GLDA}^{-} + \text{H}^+ \rightleftharpoons \text{H}_4\text{GLDA}$	20.45
HIDS		$\text{HIDS}^{4-} + \text{H}^+ \rightleftharpoons \text{HHIDS}^{3-}$	9.61
		$\text{HHIDS}^{3-} + \text{H}^+ \rightleftharpoons \text{H}_2\text{HIDS}^{2-}$	13.68
		$\text{H}_2\text{HIDS}^{2-} + \text{H}^+ \rightleftharpoons \text{H}_3\text{HIDS}^{-}$	16.76
		$\text{H}_3\text{HIDS}^{-} + \text{H}^+ \rightleftharpoons \text{H}_4\text{HIDS}$	18.90
		$\text{H}_4\text{HIDS} + \text{H}^+ \rightleftharpoons \text{H}_5\text{HIDS}^+$	20.50

^a Ionic strength, $I = 0.10 \text{ mol} \cdot \text{dm}^{-3}$; $T = 25 \text{ }^\circ\text{C}$; In aqueous matrix [35, 36].

^b The symbols p , q , and r denote, respectively, the stoichiometric coefficients for metal ions, protons, and chelators in an ML system associated with the possible equilibria in solution.

Table 2. The Overall Formation Constants ($\log_{10}\beta_{pqr}$) for M + GLDA Systems (M = Mg^{II}, Ca^{II}, Sr^{II}, or Ba^{II}) in the Aqueous Matrix ($I = 0.1 \text{ mol}\cdot\text{dm}^{-3}$; $25 \pm 0.1^\circ\text{C}$; M: L = 1:1)^a

Formation reactions	<i>p</i>	<i>q</i>	<i>r</i>	$\log_{10}\beta_{pqr}$	SD
Mg^{II}					
$\text{Mg}^{2+} + \text{OH}^- + \text{GLDA}^{4-} \rightleftharpoons \text{Mg}(\text{OH})\text{GLDA}^{3-}$	1	-1	1	-6.03	0.03
$\text{Mg}^{2+} + \text{GLDA}^{4-} \rightleftharpoons \text{MgGLDA}^{2-}$	1	0	1	5.31	0.03
Ca^{II}					
$\text{Ca}^{2+} + \text{GLDA}^{4-} \rightleftharpoons \text{CaGLDA}^{2-}$	1	0	1	5.88	0.04
Sr^{II}					
$\text{Sr}^{2+} + \text{OH}^- + \text{GLDA}^{4-} \rightleftharpoons \text{Sr}(\text{OH})\text{GLDA}^{3-}$	1	-1	1	-7.28	0.04
$\text{Sr}^{2+} + \text{GLDA}^{4-} \rightleftharpoons \text{SrGLDA}^{2-}$	1	0	1	4.04	0.04
Ba^{II}					
$\text{Ba}^{2+} + \text{OH}^- + \text{GLDA}^{4-} \rightleftharpoons \text{Ba}(\text{OH})\text{GLDA}^{3-}$	1	-1	1	-7.45	0.03
$\text{Ba}^{2+} + \text{GLDA}^{4-} \rightleftharpoons \text{BaGLDA}^{2-}$	1	0	1	3.64	0.04

^a Experimental potentiometric data were processed with HYPERQUAD 2008 to derive the $\log_{10}\beta_{pqr}$ ($n = 3$). The symbols *p*, *q*, and *r* denote, respectively, the stoichiometric coefficients for metal ions, protons, and chelators in an ML system associated with the possible equilibria in solution.

Table 3. The Overall Formation Constants ($\log_{10}\beta_{pqr}$) for M + HIDS Systems (M = Mg^{II}, Ca^{II}, Sr^{II}, or Ba^{II}) in the Aqueous Matrix ($I = 0.1 \text{ mol}\cdot\text{dm}^{-3}$; $25 \pm 0.1^\circ\text{C}$; M:L = 1:1)^a

Formation reactions	<i>p</i>	<i>q</i>	<i>r</i>	$\log_{10}\beta_{pqr}$	SD
Mg^{II}					
$\text{Mg}^{2+} + \text{OH}^- + \text{HIDS}^{4-} \rightleftharpoons \text{Mg}(\text{OH})\text{HIDS}^{3-}$	1	-1	1	-5.13	0.02
$\text{Mg}^{2+} + \text{HIDS}^{4-} \rightleftharpoons \text{MgHIDS}^{2-}$	1	0	1	5.57	0.02
Ca^{II}					
$\text{Ca}^{2+} + \text{OH}^- + \text{HIDS}^{4-} \rightleftharpoons \text{Ca}(\text{OH})\text{HIDS}^{3-}$	1	-1	1	-5.88	0.02
$\text{Ca}^{2+} + \text{HIDS}^{4-} \rightleftharpoons \text{CaHIDS}^{2-}$	1	0	1	5.05	0.02
Sr^{II}					
$\text{Sr}^{2+} + \text{OH}^- + \text{HIDS}^{4-} \rightleftharpoons \text{Sr}(\text{OH})\text{HIDS}^{3-}$	1	-1	1	-5.45	0.03
$\text{Sr}^{2+} + \text{HIDS}^{4-} \rightleftharpoons \text{SrHIDS}^{2-}$	1	0	1	4.7	0.04
Ba^{II}					
$\text{Ba}^{2+} + \text{OH}^- + \text{HIDS}^{4-} \rightleftharpoons \text{Ba}(\text{OH})\text{HIDS}^{3-}$	1	-1	1	-6.39	0.02
$\text{Ba}^{2+} + \text{HIDS}^{4-} \rightleftharpoons \text{BaHIDS}^{2-}$	1	0	1	3.8	0.03

^a Experimental potentiometric data were processed with HYPERQUAD 2008 to derive the $\log_{10}\beta_{pqr}$ ($n = 3$). The symbols *p*, *q*, and *r* denote, respectively, the stoichiometric coefficients for metal ions, protons, and chelators in an ML system associated with the possible equilibria in solution.

Table 4. The Overall Formation Constants ($\log_{10}\beta_{pqr}$) for $Y^{III} + L$ Systems ($L = \text{GLDA}$, or HIDS) in the Aqueous Matrix ($I = 0.1 \text{ mol}\cdot\text{dm}^{-3}$; $25 \pm 0.1^\circ\text{C}$; $M:L = 1:1$)^a

Formation reactions	<i>p</i>	<i>q</i>	<i>r</i>	$\log_{10}\beta_{pqr}$	SD
$Y^{III} + \text{GLDA}$					
$Y^{3+} + 2OH^- + \text{GLDA}^{4-} \rightleftharpoons Y(\text{OH})_2\text{GLDA}^{3-}$	1	-2	1	-1.43	0.06
$Y^{3+} + OH^- + \text{GLDA}^{4-} \rightleftharpoons Y(\text{OH})\text{GLDA}^{2-}$	1	-1	1	10.38	0.02
$Y^{3+} + \text{GLDA}^{4-} \rightleftharpoons Y\text{GLDA}^-$	1	0	1	14.75	0.02
$Y^{3+} + H + \text{GLDA}^{4-} \rightleftharpoons YH\text{GLDA}$	1	1	1	16.51	0.06
$Y^{III} + \text{HIDS}$					
$Y^{3+} + 3OH^- + \text{HIDS}^{4-} \rightleftharpoons Y(\text{OH})_3\text{HIDS}^{4-}$	1	-3	1	-7.72	0.02
$Y^{3+} + 2OH^- + \text{HIDS}^{4-} \rightleftharpoons Y(\text{OH})_2\text{HIDS}^{3-}$	1	-2	1	2.56	0.02
$Y^{3+} + OH^- + \text{HIDS}^{4-} \rightleftharpoons Y(\text{OH})\text{HIDS}^{2-}$	1	-1	1	9.18	0.01
$Y^{3+} + \text{HIDS}^{4-} \rightleftharpoons Y\text{HIDS}^-$	1	0	1	12.75	0.01
$Y^{3+} + H + \text{HIDS}^{4-} \rightleftharpoons YHH\text{IDS}$	1	1	1	15.72	0.01

^a Experimental potentiometric data were processed with HYPERQUAD 2008 to derive the $\log_{10}\beta_{pqr}$ ($n = 3$). The symbols *p*, *q*, and *r* denote, respectively, the stoichiometric coefficients for metal ions, protons, and chelators in an ML system associated with the possible equilibria in solution.

Table 5. The Dominant Species in the ML Systems (M = Mg^{II}, Ca^{II}, Sr^{II}, Ba^{II}, or Y^{III}; L = GLDA or HIDS) in Aqueous Matrix ($I = 0.1 \text{ mol}\cdot\text{dm}^{-3}$; $25 \pm 0.1^\circ\text{C}$; M:L = 1:1)^a

ML system	Dominant Species	pH range	%formation
Mg ^{II} + GLDA	MgGLDA ²⁻	7.4–11.3	50–92
Mg ^{II} + HIDS	MgHIDS ²⁻	7.6–10.6	50–82
Ca ^{II} + GLDA	CaGLDA ²⁻	6.5–12	50–98
Ca ^{II} + HIDS	CaHIDS ²⁻	7.8–10.9	50–89
Sr ^{II} + GLDA	SrGLDA ²⁻	8.7–11.1	50–70
Sr ^{II} + HIDS	SrHIDS ²⁻	8.5–10	50–64
Ba ^{II} + GLDA	BaGLDA ²⁻	9.0–10.7	50–60
Ba ^{II} + HIDS	BaHIDS ²⁻	9.0–10	40–46
Y ^{III} + GLDA	Y(OH)GLDA ²⁻	4.4–11.8	50–99
Y ^{III} + HIDS	Y(OH)HIDS ²⁻	3.7–6.6	50–94
	Y(OH) ₂ HIDS ³⁻	6.6–10.3	50–96

^a Experimental potentiometric data were processed with HYPERQUAD 2008 to derive the species distribution information in the ML systems.

Table 6. The protonation and complexation of the GLDA and HIDS with the metal ions (Mg^{II} , Ca^{II} , Sr^{II} , Ba^{II} , or Y^{III}) compared with the corresponding values of EDDS and EDTA in the aqueous matrix ($I = 0.1 \text{ mol}\cdot\text{dm}^{-3}$; $25 \pm 0.1^\circ\text{C}$; $\text{M:L} = 1:1$)^a

Equilibria	GLDA (H_4L) ^{§, a}	HIDS (H_4L) ^a	EDDS (H_4L) ^b	EDTA (H_4L) ^b
	$\log_{10}K$	$\log_{10}K$	$\log_{10}K$	$\log_{10}K$
[HL]/[H][L]	9.39 (9.36)	9.61	10.01	9.52–10.37
[H ₂ L]/[HL][H]	5.01 (5.03)	4.07	6.84	6.13
[H ₃ L]/[H ₂ L][H]	3.49 (3.49)	3.08	3.86	2.69
[H ₄ L]/[H ₃ L][H]	2.56 (2.56)	2.14	2.95	2
[H ₅ L]/[H ₄ L][H]	–	(1.6)	–	(1.5)
[H ₆ L]/[H ₅ L][H]	–	–	–	(0.0)
Mg^{II}				
[ML]/[MOHL][H]	11.34	10.71	–	–
[ML]/[M][L]	5.31 (5.18)	5.57	6.01	8.96
[MHL]/[ML][H]	–	–	(1.8) ^c	4
Ca^{II}				
[ML]/[MOHL][H]	–	10.93	–	–
[ML]/[M][L]	5.88 (5.93)	5.05	4.58	10.81
[MHL]/[ML][H]	–	–	(1.4)	3.1
Sr^{II}				
[ML]/[MOHL][H]	11.32	10.16	–	–
[ML]/[M][L]	4.04 (4.06)	4.7	3.7	8.72
[MHL]/[ML][H]	–	–	(1.3)	3.93 ^c
Ba^{II}				
[ML]/[MOHL][H]	11.08	10.19	–	–
[ML]/[M][L]	3.64 (3.54)	3.8	3	7.88
[MHL]/[ML][H]	–	–	(1)	–
Y^{III}				
[M(OH) ₂ L]/[M(OH) ₃ L][H]	–	10.28	–	–
[M(OH)L]/[M(OH) ₂ L][H]	11.81	6.62	–	–
[M(L)/[MOHL][H]	4.37	3.57	–	–
[ML]/[M][L]	14.75	12.75	13.55	18.08
[MHL]/[ML][H]	1.76	2.96	–	–

[§]The data in the parenthesis were reported in the NIST critically selected stability constants of metal complexes database [41].

^a Experimental potentiometric data were processed with HYPERQUAD 2008 to derive the $\log_{10}\beta_{pq}$ ($n = 3$).

^b Data source: NIST critically selected stability constants of metal complexes database [41].

^c $T = 20^\circ\text{C}$.

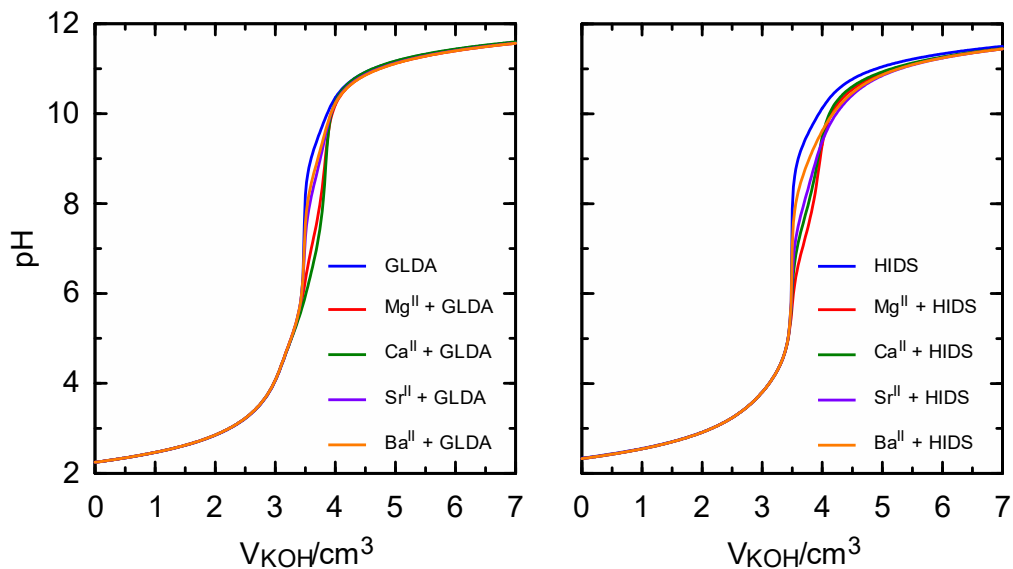


Figure 1: Potentiometric titration curves for the ML systems ($M = \text{Mg}^{\text{II}}$, Ca^{II} , Sr^{II} , or Ba^{II} ; $L = \text{GLDA}$ or HIDS) as a function of titer volume in the aqueous matrix ($I = 0.1 \text{ mol}\cdot\text{dm}^{-3}$; $T = 25 \pm 0.1^\circ\text{C}$; $M:L = 1:1$).

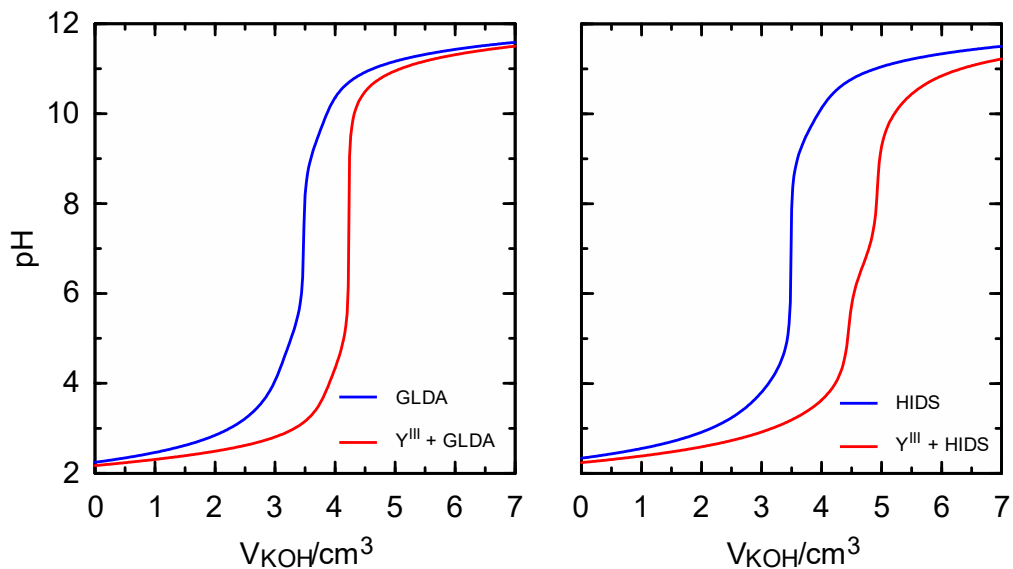


Figure 2: Potentiometric titration curves for the Y^{III} -L systems (L = GLDA or HIDS) as a function of titer volume in the aqueous matrix ($I = 0.1 \text{ mol} \cdot \text{dm}^{-3}$; $T = 25 \pm 0.1^\circ\text{C}$; M:L = 1:1).

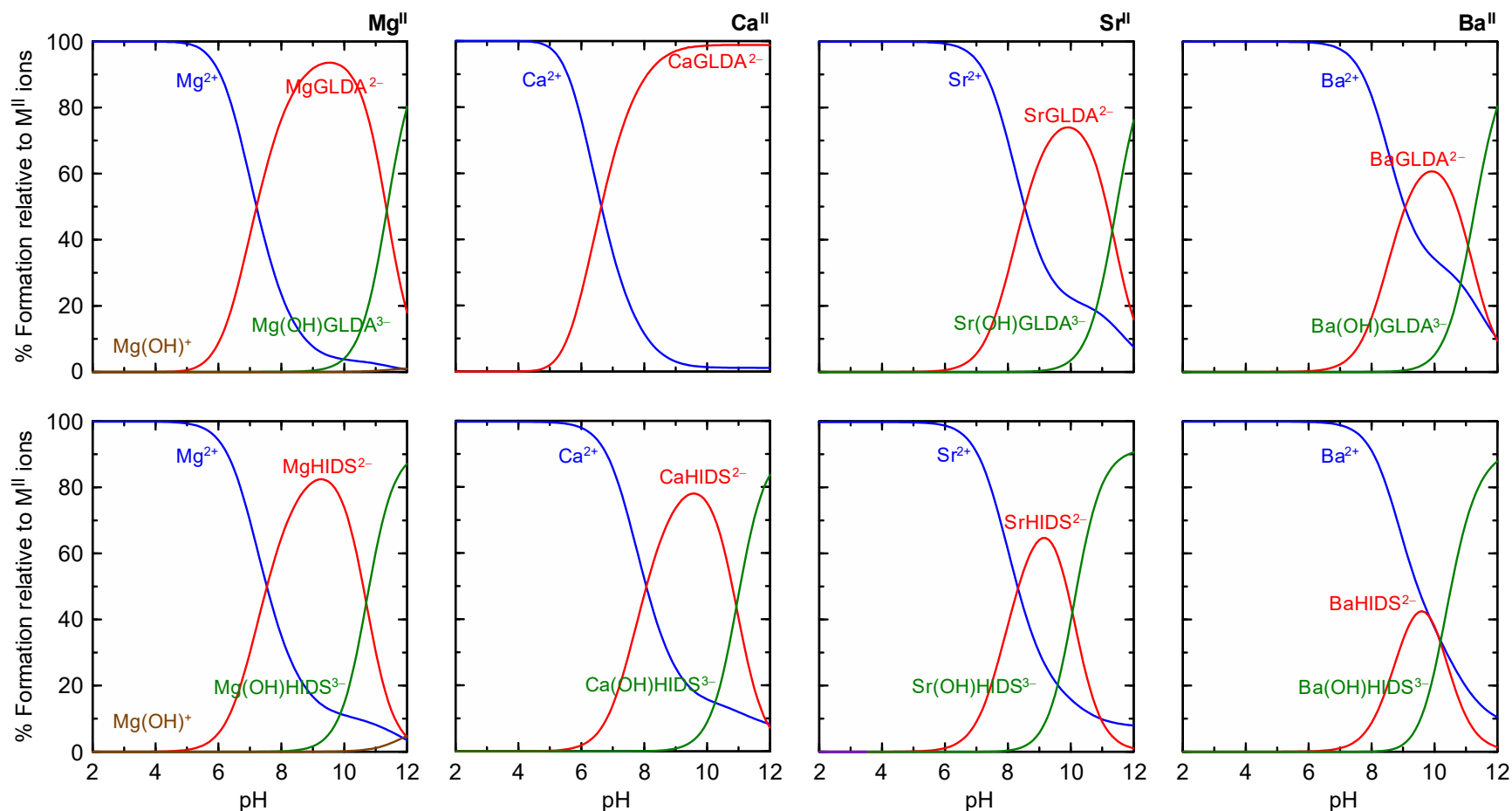


Figure 3. The species distribution curves for the ML systems (M = Mg^{II}, Ca^{II}, Sr^{II}, or Ba^{II}; L = GLDA or HIDS) as a function of pH in the aqueous matrix ($I = 0.1 \text{ mol} \cdot \text{dm}^{-3}$; $T = 25 \pm 0.1^\circ\text{C}$; M:L = 1:1).

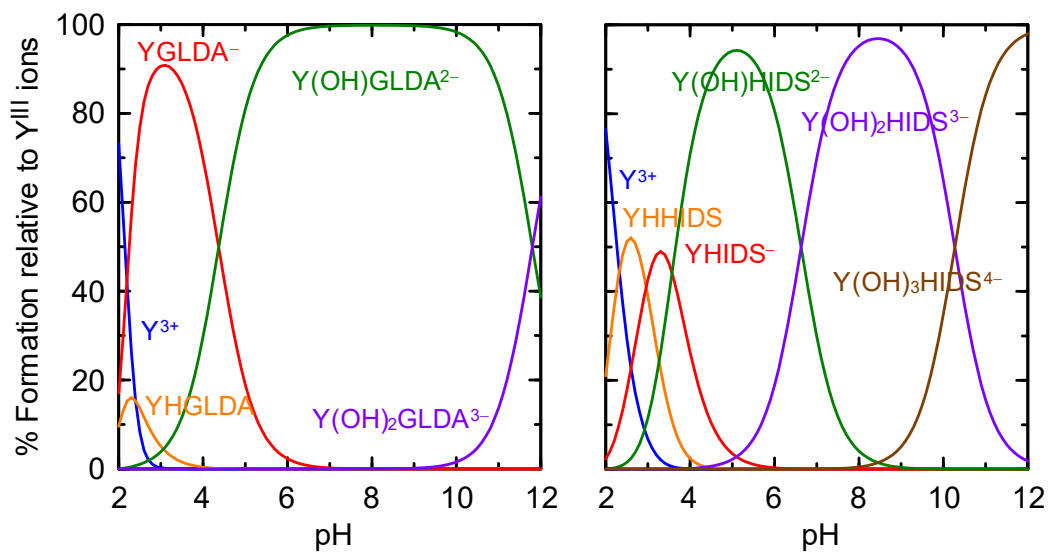


Figure 4: The species distribution curves for the Y^{III}-L systems (L = GLDA or HIDS) as a function of pH in the aqueous matrix ($I = 0.1 \text{ mol} \cdot \text{dm}^{-3}$; $T = 25 \pm 0.1^\circ\text{C}$; M:L = 1:1).

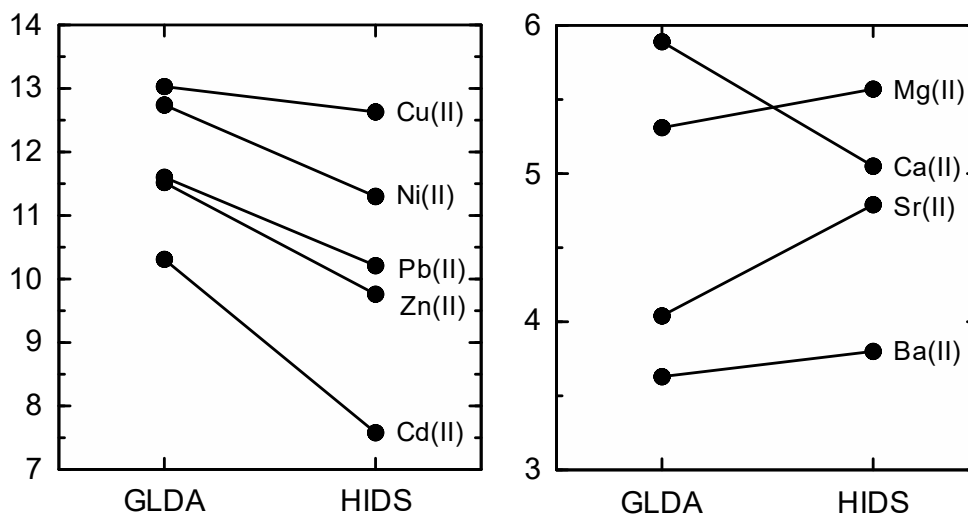


Figure 5: A comparison in the stability trend between M-GLDA and M-HIDS complexes in the aqueous matrix (M = Mg, Ca, Sr, Ba, Ni, Cu, Zn, Cd, or Pb; $I = 0.1 \text{ mol}\cdot\text{dm}^{-3}$; $T = 25 \pm 0.1^\circ\text{C}$; M:L = 1:1).

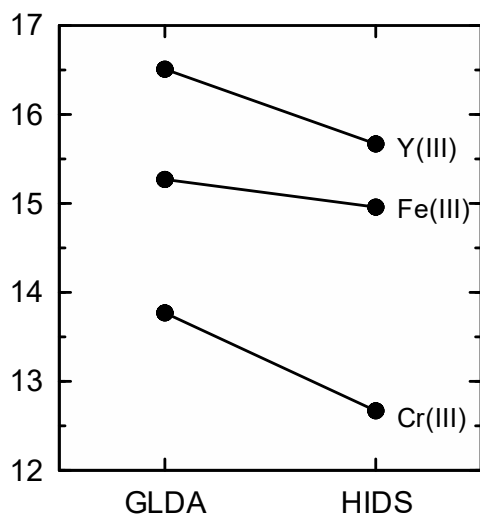


Figure 6: A comparison in the stability trend between M-GLDA and M-HIDS complexes in the aqueous matrix ($M = \text{Cr}^{\text{III}}$, Fe^{III} , or Y^{III} ; $I = 0.1 \text{ mol} \cdot \text{dm}^{-3}$; $T = 25 \pm 0.1^\circ\text{C}$; $M:L = 1:1$).

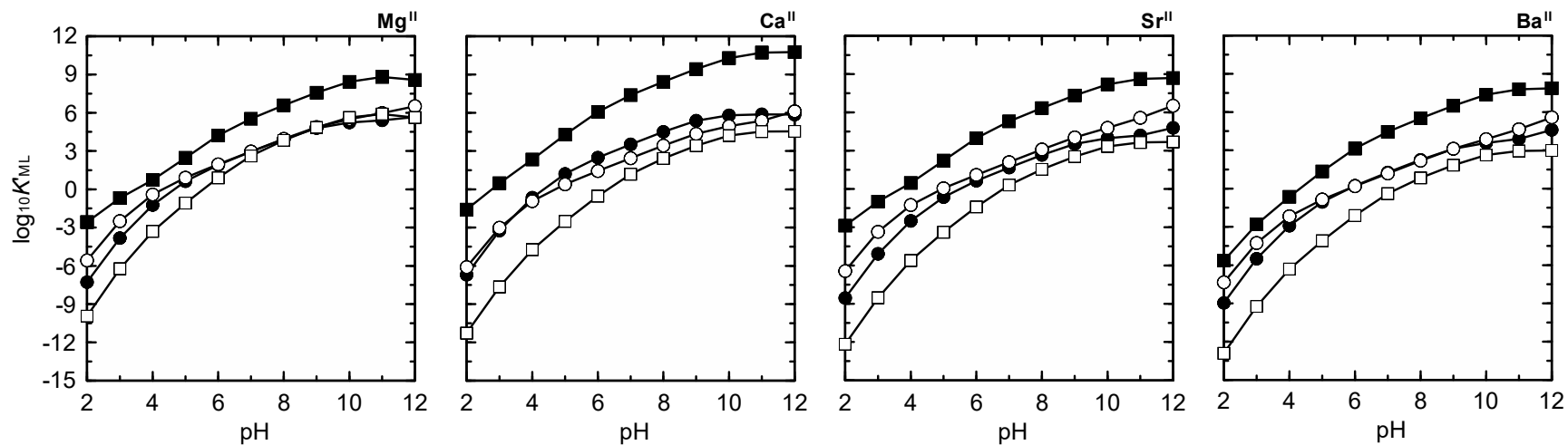


Figure 7: The comparative conditional stability constants ($\log_{10}K'_{ML}$) for the ML systems ($M = \text{Mg}^{\text{II}}$, Ca^{II} , Sr^{II} , or Ba^{II} ; $L = \text{GLDA}$, HIDS , EDDS or EDTA) as a function of pH in the aqueous matrix ($I = 0.1 \text{ mol}\cdot\text{dm}^{-3}$; $T = 25 \pm 0.1^\circ\text{C}$; $M:L = 1:1$): ●, M-GLDA; ○, M-HIDS; □, M-EDDS; ■, M-EDTA.

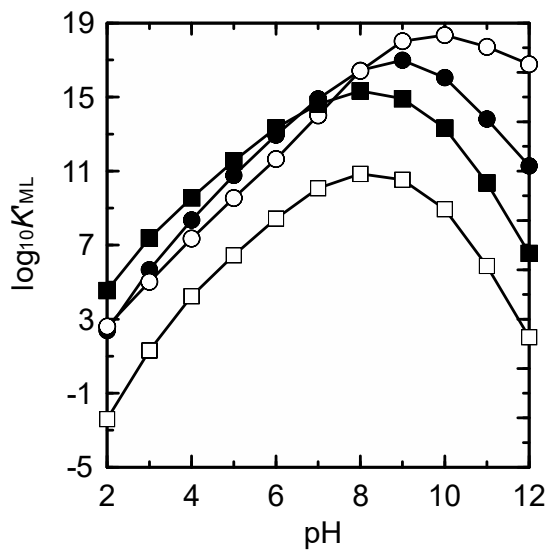


Figure 8: The comparative conditional stability constants ($\log_{10}K'_{ML}$) for the Y^{III} -L systems (L = GLDA, HIDS, EDDS or EDTA) as a function of pH in the aqueous matrix ($I = 0.1 \text{ mol}\cdot\text{dm}^{-3}$; $T = 25 \pm 0.1^\circ\text{C}$; M:L = 1:1): ●, Y^{III} -GLDA; ○, Y^{III} -HIDS; □, Y^{III} -EDDS; ■, Y^{III} -EDTA.

Appendix A. Supplementary Data

Complexation Behavior of Sr^{II} and Geochemically-Related Elements (Mg^{II}, Ca^{II}, Ba^{II}, and Y^{III}) with Biodegradable Aminopolycarboxylate Chelators (GLDA and HIDS)

Zinnat A. Begum,^{1, 2, †, *} Ismail M. M. Rahman,^{1, †, *} Hiroshi Hasegawa³

¹*Institute of Environmental Radioactivity, Fukushima University, 1 Kanayagawa, Fukushima City, Fukushima 960-1296, Japan*

²*Department of Civil Engineering, Southern University, 739/A Mehedibag Road, Chittagong 4000, Bangladesh*

³*Institute of Science and Engineering, Kanazawa University, Kakuma, Kanazawa 920-1192, Japan*

†Co-First Author

*Corresponding authors

E-mail: zinnat.ara@gmail.com (ZAB); i.m.m.rahman@gmail.com (IMMR)

Appendix A. Supplementary Data

Supplementary Data

Contents	Page No.
Table S1 Potentiometric Titration Data for the ML systems (M = Mg ^{II} , Ca ^{II} , Sr ^{II} , and Ba ^{II} ; L = GLDA) in the Aqueous Matrix ($I = 0.1 \text{ mol} \cdot \text{dm}^{-3}$; $25 \pm 0.1^\circ\text{C}$; M:L = 1:1)	S-3
Table S2 Potentiometric Titration Data for the ML systems (M = Mg ^{II} , Ca ^{II} , Sr ^{II} , and Ba ^{II} ; L = HIDS) in the Aqueous Matrix ($I = 0.1 \text{ mol} \cdot \text{dm}^{-3}$; $25 \pm 0.1^\circ\text{C}$; M:L = 1:1)	S-11
Table S3 Potentiometric Titration Data for the ML systems (M = Y ^{III} ; L = GLDA and HIDS) in the Aqueous Matrix ($I = 0.1 \text{ mol} \cdot \text{dm}^{-3}$; $25 \pm 0.1^\circ\text{C}$; M:L = 1:1)	S-19

Appendix A. Supplementary Data

Table S1: Potentiometric Titration Data for the ML systems (M = Mg^{II}, Ca^{II}, Sr^{II}, and Ba^{II}; L = GLDA) in the Aqueous Matrix ($I = 0.1 \text{ mol}\cdot\text{dm}^{-3}$; $25 \pm 0.1^\circ\text{C}$; M:L = 1:1)

Sl	V _{KOH} /cm ³	GLDA	Mg ^{II} + GLDA	Ca ^{II} + GLDA	Sr ^{II} + GLDA	Ba ^{II} + GLDA
1	0.00	2.243	2.244	2.244	2.244	2.244
2	0.02	2.247	2.248	2.248	2.248	2.248
3	0.04	2.250	2.251	2.251	2.251	2.251
4	0.06	2.254	2.255	2.255	2.255	2.255
5	0.08	2.257	2.259	2.259	2.259	2.259
6	0.10	2.261	2.262	2.262	2.262	2.262
7	0.12	2.265	2.266	2.266	2.266	2.266
8	0.14	2.269	2.270	2.270	2.270	2.270
9	0.16	2.272	2.274	2.274	2.274	2.274
10	0.18	2.276	2.277	2.277	2.277	2.277
11	0.20	2.280	2.281	2.281	2.281	2.281
12	0.22	2.284	2.285	2.285	2.285	2.285
13	0.24	2.288	2.289	2.289	2.289	2.289
14	0.26	2.292	2.293	2.293	2.293	2.293
15	0.28	2.296	2.297	2.297	2.297	2.297
16	0.30	2.299	2.301	2.301	2.301	2.301
17	0.32	2.303	2.305	2.305	2.305	2.305
18	0.34	2.308	2.309	2.309	2.309	2.309
19	0.36	2.312	2.313	2.313	2.313	2.313
20	0.38	2.316	2.317	2.317	2.317	2.317
21	0.40	2.320	2.321	2.321	2.321	2.321
22	0.42	2.324	2.325	2.325	2.325	2.325
23	0.44	2.328	2.330	2.330	2.330	2.330
24	0.46	2.332	2.334	2.334	2.334	2.334
25	0.48	2.337	2.338	2.338	2.338	2.338
26	0.50	2.341	2.342	2.342	2.342	2.342
27	0.52	2.345	2.347	2.347	2.347	2.347
28	0.54	2.350	2.351	2.351	2.351	2.351
29	0.56	2.354	2.356	2.356	2.356	2.356
30	0.58	2.359	2.360	2.360	2.360	2.360
31	0.60	2.363	2.365	2.365	2.365	2.365
32	0.62	2.368	2.369	2.369	2.369	2.369
33	0.64	2.372	2.374	2.374	2.374	2.374
34	0.66	2.377	2.378	2.378	2.378	2.378
35	0.68	2.381	2.383	2.383	2.383	2.383
36	0.70	2.386	2.388	2.388	2.388	2.388
37	0.72	2.391	2.393	2.393	2.393	2.393
38	0.74	2.396	2.397	2.397	2.397	2.397
39	0.76	2.400	2.402	2.402	2.402	2.402
40	0.78	2.405	2.407	2.407	2.407	2.407
41	0.80	2.410	2.412	2.412	2.412	2.412
42	0.82	2.415	2.417	2.417	2.417	2.417

Appendix A. Supplementary Data

Sl	$V_{\text{KOH}}/\text{cm}^3$	GLDA	$\text{Mg}^{\text{II}} + \text{GLDA}$	$\text{Ca}^{\text{II}} + \text{GLDA}$	$\text{Sr}^{\text{II}} + \text{GLDA}$	$\text{Ba}^{\text{II}} + \text{GLDA}$
43	0.84	2.420	2.422	2.422	2.422	2.422
44	0.86	2.425	2.427	2.427	2.427	2.427
45	0.88	2.430	2.432	2.432	2.432	2.432
46	0.90	2.435	2.438	2.438	2.438	2.438
47	0.92	2.441	2.443	2.443	2.443	2.443
48	0.94	2.446	2.448	2.448	2.448	2.448
49	0.96	2.451	2.453	2.453	2.453	2.453
50	0.98	2.457	2.459	2.459	2.459	2.459
51	1.00	2.462	2.464	2.464	2.464	2.464
52	1.02	2.468	2.470	2.470	2.470	2.470
53	1.04	2.473	2.475	2.475	2.475	2.475
54	1.06	2.479	2.481	2.481	2.481	2.481
55	1.08	2.484	2.487	2.487	2.487	2.487
56	1.10	2.490	2.493	2.493	2.493	2.493
57	1.12	2.496	2.498	2.498	2.498	2.498
58	1.14	2.502	2.504	2.504	2.504	2.504
59	1.16	2.508	2.510	2.510	2.510	2.510
60	1.18	2.514	2.516	2.516	2.516	2.516
61	1.20	2.520	2.522	2.522	2.522	2.522
62	1.22	2.526	2.529	2.529	2.529	2.529
63	1.24	2.532	2.535	2.535	2.535	2.535
64	1.26	2.538	2.541	2.541	2.541	2.541
65	1.28	2.545	2.547	2.547	2.547	2.547
66	1.30	2.551	2.554	2.554	2.554	2.554
67	1.32	2.558	2.561	2.561	2.561	2.561
68	1.34	2.564	2.567	2.567	2.567	2.567
69	1.36	2.571	2.574	2.574	2.574	2.574
70	1.38	2.578	2.581	2.581	2.581	2.581
71	1.40	2.585	2.588	2.588	2.588	2.588
72	1.42	2.592	2.595	2.595	2.595	2.595
73	1.44	2.599	2.602	2.602	2.602	2.602
74	1.46	2.606	2.609	2.609	2.609	2.609
75	1.48	2.613	2.616	2.616	2.616	2.616
76	1.50	2.620	2.624	2.624	2.624	2.624
77	1.52	2.628	2.631	2.631	2.631	2.631
78	1.54	2.635	2.639	2.639	2.639	2.639
79	1.56	2.643	2.646	2.646	2.646	2.646
80	1.58	2.651	2.654	2.654	2.654	2.654
81	1.60	2.659	2.662	2.662	2.662	2.662
82	1.62	2.666	2.670	2.670	2.670	2.670
83	1.64	2.675	2.678	2.678	2.678	2.678
84	1.66	2.683	2.687	2.687	2.687	2.687
85	1.68	2.691	2.695	2.695	2.695	2.695
86	1.70	2.700	2.704	2.704	2.704	2.704
87	1.72	2.708	2.712	2.712	2.712	2.712

Appendix A. Supplementary Data

SI	$V_{\text{KOH}}/\text{cm}^3$	GLDA	$\text{Mg}^{\text{II}} + \text{GLDA}$	$\text{Ca}^{\text{II}} + \text{GLDA}$	$\text{Sr}^{\text{II}} + \text{GLDA}$	$\text{Ba}^{\text{II}} + \text{GLDA}$
88	1.74	2.717	2.721	2.721	2.721	2.721
89	1.76	2.726	2.730	2.730	2.730	2.730
90	1.78	2.735	2.739	2.739	2.739	2.739
91	1.80	2.744	2.748	2.748	2.748	2.748
92	1.82	2.753	2.758	2.758	2.758	2.758
93	1.84	2.763	2.767	2.767	2.767	2.767
94	1.86	2.773	2.777	2.777	2.777	2.777
95	1.88	2.782	2.787	2.787	2.787	2.787
96	1.90	2.792	2.797	2.797	2.797	2.797
97	1.92	2.803	2.807	2.807	2.807	2.807
98	1.94	2.813	2.818	2.818	2.818	2.818
99	1.96	2.824	2.829	2.829	2.829	2.829
100	1.98	2.834	2.840	2.840	2.840	2.840
101	2.00	2.845	2.851	2.851	2.851	2.851
102	2.02	2.857	2.862	2.862	2.862	2.862
103	2.04	2.868	2.873	2.873	2.873	2.873
104	2.06	2.880	2.885	2.885	2.885	2.885
105	2.08	2.892	2.897	2.897	2.897	2.897
106	2.10	2.904	2.909	2.909	2.909	2.909
107	2.12	2.916	2.922	2.922	2.922	2.922
108	2.14	2.929	2.935	2.935	2.935	2.935
109	2.16	2.942	2.948	2.948	2.948	2.948
110	2.18	2.955	2.961	2.961	2.961	2.961
111	2.20	2.968	2.975	2.975	2.975	2.975
112	2.22	2.982	2.989	2.989	2.989	2.989
113	2.24	2.996	3.003	3.003	3.003	3.003
114	2.26	3.011	3.018	3.018	3.018	3.018
115	2.28	3.026	3.033	3.033	3.033	3.033
116	2.30	3.041	3.048	3.048	3.048	3.048
117	2.32	3.057	3.064	3.064	3.064	3.064
118	2.34	3.072	3.080	3.080	3.080	3.080
119	2.36	3.089	3.096	3.096	3.096	3.096
120	2.38	3.106	3.113	3.113	3.113	3.113
121	2.40	3.123	3.131	3.131	3.131	3.131
122	2.42	3.141	3.149	3.149	3.149	3.149
123	2.44	3.159	3.167	3.167	3.167	3.167
124	2.46	3.178	3.186	3.186	3.186	3.186
125	2.48	3.197	3.206	3.206	3.206	3.206
126	2.50	3.217	3.226	3.226	3.226	3.226
127	2.52	3.237	3.246	3.246	3.246	3.246
128	2.54	3.258	3.268	3.268	3.268	3.268
129	2.56	3.280	3.290	3.290	3.290	3.290
130	2.58	3.303	3.312	3.312	3.312	3.312
131	2.60	3.326	3.336	3.336	3.336	3.336
132	2.62	3.350	3.360	3.360	3.360	3.360

Appendix A. Supplementary Data

Sl	$V_{\text{KOH}}/\text{cm}^3$	GLDA	$\text{Mg}^{\text{II}} + \text{GLDA}$	$\text{Ca}^{\text{II}} + \text{GLDA}$	$\text{Sr}^{\text{II}} + \text{GLDA}$	$\text{Ba}^{\text{II}} + \text{GLDA}$
133	2.64	3.375	3.385	3.385	3.385	3.385
134	2.66	3.400	3.411	3.411	3.411	3.411
135	2.68	3.427	3.438	3.438	3.438	3.438
136	2.70	3.455	3.466	3.466	3.466	3.466
137	2.72	3.483	3.494	3.494	3.494	3.494
138	2.74	3.513	3.525	3.525	3.525	3.525
139	2.76	3.544	3.556	3.556	3.556	3.556
140	2.78	3.577	3.588	3.588	3.588	3.588
141	2.80	3.610	3.623	3.623	3.623	3.623
142	2.82	3.646	3.658	3.658	3.658	3.658
143	2.84	3.683	3.695	3.695	3.695	3.695
144	2.86	3.722	3.735	3.734	3.735	3.735
145	2.88	3.762	3.776	3.776	3.776	3.776
146	2.90	3.805	3.819	3.819	3.819	3.819
147	2.92	3.851	3.864	3.864	3.865	3.865
148	2.94	3.899	3.913	3.912	3.913	3.913
149	2.96	3.949	3.964	3.963	3.964	3.964
150	2.98	4.003	4.017	4.017	4.017	4.017
151	3.00	4.059	4.074	4.074	4.074	4.074
152	3.02	4.119	4.134	4.134	4.135	4.135
153	3.04	4.182	4.197	4.197	4.198	4.198
154	3.06	4.248	4.263	4.262	4.264	4.264
155	3.08	4.316	4.332	4.330	4.333	4.333
156	3.10	4.386	4.403	4.400	4.403	4.403
157	3.12	4.458	4.475	4.471	4.476	4.476
158	3.14	4.531	4.547	4.543	4.549	4.549
159	3.16	4.604	4.621	4.615	4.623	4.623
160	3.18	4.678	4.694	4.686	4.696	4.696
161	3.20	4.752	4.767	4.758	4.770	4.770
162	3.22	4.826	4.840	4.828	4.844	4.844
163	3.24	4.900	4.913	4.898	4.919	4.919
164	3.26	4.976	4.987	4.968	4.994	4.995
165	3.28	5.053	5.062	5.038	5.071	5.072
166	3.30	5.132	5.139	5.109	5.151	5.151
167	3.32	5.216	5.219	5.181	5.234	5.235
168	3.34	5.305	5.302	5.254	5.323	5.324
169	3.36	5.402	5.391	5.329	5.420	5.421
170	3.38	5.510	5.486	5.407	5.527	5.529
171	3.40	5.637	5.590	5.488	5.652	5.655
172	3.42	5.793	5.706	5.572	5.804	5.809
173	3.44	6.007	5.836	5.660	6.007	6.018
174	3.46	6.372	5.980	5.752	6.315	6.356
175	3.48	7.507	6.135	5.848	6.810	7.028
176	3.50	8.192	6.295	5.947	7.248	7.562
177	3.52	8.473	6.451	6.049	7.524	7.847

Appendix A. Supplementary Data

SI	$V_{\text{KOH}}/\text{cm}^3$	GLDA	$\text{Mg}^{\text{II}} + \text{GLDA}$	$\text{Ca}^{\text{II}} + \text{GLDA}$	$\text{Sr}^{\text{II}} + \text{GLDA}$	$\text{Ba}^{\text{II}} + \text{GLDA}$
178	3.54	8.658	6.600	6.153	7.725	8.046
179	3.56	8.800	6.740	6.260	7.888	8.203
180	3.58	8.918	6.874	6.369	8.030	8.337
181	3.60	9.021	7.003	6.480	8.158	8.457
182	3.62	9.114	7.130	6.594	8.279	8.568
183	3.64	9.199	7.257	6.711	8.394	8.672
184	3.66	9.280	7.385	6.834	8.505	8.772
185	3.68	9.358	7.518	6.963	8.616	8.869
186	3.70	9.433	7.657	7.101	8.726	8.965
187	3.72	9.506	7.805	7.250	8.836	9.060
188	3.74	9.578	7.966	7.416	8.949	9.155
189	3.76	9.649	8.143	7.604	9.064	9.252
190	3.78	9.719	8.342	7.823	9.182	9.349
191	3.80	9.788	8.568	8.089	9.302	9.447
192	3.82	9.857	8.821	8.424	9.425	9.545
193	3.84	9.923	9.090	8.834	9.547	9.642
194	3.86	9.988	9.345	9.243	9.665	9.736
195	3.88	10.050	9.560	9.551	9.775	9.825
196	3.90	10.109	9.729	9.763	9.876	9.909
197	3.92	10.165	9.861	9.915	9.966	9.985
198	3.94	10.217	9.968	10.031	10.046	10.055
199	3.96	10.266	10.056	10.124	10.117	10.119
200	3.98	10.312	10.130	10.201	10.180	10.176
201	4.00	10.355	10.195	10.267	10.236	10.229
202	4.02	10.396	10.251	10.325	10.287	10.277
203	4.04	10.433	10.302	10.375	10.333	10.321
204	4.06	10.468	10.347	10.421	10.375	10.362
205	4.08	10.501	10.389	10.462	10.414	10.400
206	4.10	10.532	10.426	10.500	10.450	10.435
207	4.12	10.562	10.461	10.535	10.483	10.468
208	4.14	10.589	10.494	10.567	10.514	10.498
209	4.16	10.616	10.524	10.597	10.543	10.527
210	4.18	10.640	10.553	10.625	10.571	10.554
211	4.20	10.664	10.579	10.651	10.597	10.580
212	4.22	10.687	10.604	10.676	10.621	10.605
213	4.24	10.708	10.628	10.699	10.645	10.628
214	4.26	10.729	10.651	10.721	10.667	10.650
215	4.28	10.748	10.673	10.742	10.688	10.672
216	4.30	10.767	10.693	10.763	10.708	10.692
217	4.32	10.785	10.713	10.782	10.727	10.711
218	4.34	10.802	10.732	10.800	10.746	10.730
219	4.36	10.819	10.750	10.818	10.764	10.748
220	4.38	10.835	10.767	10.835	10.781	10.765
221	4.40	10.851	10.784	10.851	10.797	10.782
222	4.42	10.866	10.800	10.867	10.813	10.798

Appendix A. Supplementary Data

SI	$V_{\text{KOH}}/\text{cm}^3$	GLDA	$\text{Mg}^{\text{II}} + \text{GLDA}$	$\text{Ca}^{\text{II}} + \text{GLDA}$	$\text{Sr}^{\text{II}} + \text{GLDA}$	$\text{Ba}^{\text{II}} + \text{GLDA}$
223	4.44	10.881	10.816	10.882	10.829	10.814
224	4.46	10.895	10.831	10.897	10.844	10.829
225	4.48	10.908	10.846	10.911	10.858	10.843
226	4.50	10.922	10.860	10.924	10.872	10.857
227	4.52	10.934	10.874	10.938	10.885	10.871
228	4.54	10.947	10.887	10.950	10.899	10.884
229	4.56	10.959	10.900	10.963	10.911	10.897
230	4.58	10.971	10.912	10.975	10.924	10.910
231	4.60	10.982	10.925	10.987	10.936	10.922
232	4.62	10.993	10.936	10.998	10.948	10.934
233	4.64	11.004	10.948	11.009	10.959	10.946
234	4.66	11.015	10.959	11.020	10.970	10.957
235	4.68	11.025	10.970	11.031	10.981	10.968
236	4.70	11.036	10.981	11.041	10.992	10.979
237	4.72	11.045	10.992	11.051	11.002	10.990
238	4.74	11.055	11.002	11.061	11.012	11.000
239	4.76	11.065	11.012	11.071	11.022	11.010
240	4.78	11.074	11.022	11.080	11.032	11.020
241	4.80	11.083	11.031	11.090	11.041	11.030
242	4.82	11.092	11.041	11.099	11.051	11.039
243	4.84	11.100	11.050	11.107	11.060	11.048
244	4.86	11.109	11.059	11.116	11.069	11.057
245	4.88	11.117	11.068	11.124	11.077	11.066
246	4.90	11.126	11.077	11.133	11.086	11.075
247	4.92	11.134	11.085	11.141	11.094	11.084
248	4.94	11.141	11.093	11.149	11.103	11.092
249	4.96	11.149	11.102	11.157	11.111	11.100
250	4.98	11.157	11.110	11.164	11.119	11.108
251	5.00	11.164	11.118	11.172	11.126	11.116
252	5.02	11.172	11.125	11.179	11.134	11.124
253	5.04	11.179	11.133	11.187	11.142	11.132
254	5.06	11.186	11.140	11.194	11.149	11.139
255	5.08	11.193	11.148	11.201	11.156	11.147
256	5.10	11.200	11.155	11.208	11.164	11.154
257	5.12	11.207	11.162	11.215	11.171	11.161
258	5.14	11.213	11.169	11.221	11.178	11.168
259	5.16	11.220	11.176	11.228	11.184	11.175
260	5.18	11.226	11.183	11.234	11.191	11.182
261	5.20	11.232	11.190	11.241	11.198	11.189
262	5.22	11.239	11.196	11.247	11.204	11.196
263	5.24	11.245	11.203	11.253	11.211	11.202
264	5.26	11.251	11.209	11.259	11.217	11.209
265	5.28	11.257	11.215	11.265	11.223	11.215
266	5.30	11.263	11.222	11.271	11.229	11.221
267	5.32	11.269	11.228	11.277	11.235	11.227

Appendix A. Supplementary Data

SI	$V_{\text{KOH}}/\text{cm}^3$	GLDA	$\text{Mg}^{\text{II}} + \text{GLDA}$	$\text{Ca}^{\text{II}} + \text{GLDA}$	$\text{Sr}^{\text{II}} + \text{GLDA}$	$\text{Ba}^{\text{II}} + \text{GLDA}$
268	5.34	11.274	11.234	11.283	11.241	11.233
269	5.36	11.280	11.240	11.289	11.247	11.239
270	5.38	11.286	11.246	11.294	11.253	11.245
271	5.40	11.291	11.252	11.300	11.259	11.251
272	5.42	11.296	11.257	11.305	11.265	11.257
273	5.44	11.302	11.263	11.311	11.270	11.263
274	5.46	11.307	11.269	11.316	11.276	11.268
275	5.48	11.312	11.274	11.321	11.281	11.274
276	5.50	11.317	11.279	11.326	11.287	11.279
277	5.52	11.323	11.285	11.331	11.292	11.285
278	5.54	11.328	11.290	11.336	11.297	11.290
279	5.56	11.333	11.295	11.341	11.302	11.295
280	5.58	11.337	11.301	11.346	11.308	11.301
281	5.60	11.342	11.306	11.351	11.313	11.306
282	5.62	11.347	11.311	11.356	11.318	11.311
283	5.64	11.352	11.316	11.361	11.323	11.316
284	5.66	11.357	11.321	11.366	11.327	11.321
285	5.68	11.361	11.326	11.370	11.332	11.326
286	5.70	11.366	11.330	11.375	11.337	11.331
287	5.72	11.370	11.335	11.379	11.342	11.336
288	5.74	11.375	11.340	11.384	11.347	11.340
289	5.76	11.379	11.345	11.388	11.351	11.345
290	5.78	11.384	11.349	11.393	11.356	11.350
291	5.80	11.388	11.354	11.397	11.360	11.354
292	5.82	11.392	11.358	11.401	11.365	11.359
293	5.84	11.396	11.363	11.406	11.369	11.363
294	5.86	11.401	11.367	11.410	11.374	11.368
295	5.88	11.405	11.372	11.414	11.378	11.372
296	5.90	11.409	11.376	11.418	11.382	11.377
297	5.92	11.413	11.380	11.422	11.387	11.381
298	5.94	11.417	11.385	11.426	11.391	11.385
299	5.96	11.421	11.389	11.430	11.395	11.389
300	5.98	11.425	11.393	11.434	11.399	11.394
301	6.00	11.429	11.397	11.438	11.403	11.398
302	6.02	11.433	11.401	11.442	11.407	11.402
303	6.04	11.437	11.405	11.446	11.411	11.406
304	6.06	11.440	11.409	11.450	11.415	11.410
305	6.08	11.444	11.413	11.454	11.419	11.414
306	6.10	11.448	11.417	11.457	11.423	11.418
307	6.12	11.452	11.421	11.461	11.427	11.422
308	6.14	11.455	11.425	11.465	11.431	11.426
309	6.16	11.459	11.429	11.468	11.435	11.430
310	6.18	11.463	11.433	11.472	11.438	11.433
311	6.20	11.466	11.436	11.475	11.442	11.437
312	6.22	11.470	11.440	11.479	11.446	11.441

Appendix A. Supplementary Data

Sl	$V_{\text{KOH}}/\text{cm}^3$	GLDA	$\text{Mg}^{\text{II}} + \text{GLDA}$	$\text{Ca}^{\text{II}} + \text{GLDA}$	$\text{Sr}^{\text{II}} + \text{GLDA}$	$\text{Ba}^{\text{II}} + \text{GLDA}$
313	6.24	11.473	11.444	11.483	11.449	11.445
314	6.26	11.477	11.448	11.486	11.453	11.448
315	6.28	11.480	11.451	11.489	11.457	11.452
316	6.30	11.483	11.455	11.493	11.460	11.456
317	6.32	11.487	11.458	11.496	11.464	11.459
318	6.34	11.490	11.462	11.500	11.467	11.463
319	6.36	11.494	11.465	11.503	11.471	11.466
320	6.38	11.497	11.469	11.506	11.474	11.470
321	6.40	11.500	11.472	11.510	11.478	11.473
322	6.42	11.503	11.476	11.513	11.481	11.477
323	6.44	11.507	11.479	11.516	11.484	11.480
324	6.46	11.510	11.483	11.519	11.488	11.483
325	6.48	11.513	11.486	11.522	11.491	11.487
326	6.50	11.516	11.489	11.526	11.494	11.490
327	6.52	11.519	11.493	11.529	11.498	11.493
328	6.54	11.522	11.496	11.532	11.501	11.497
329	6.56	11.525	11.499	11.535	11.504	11.500
330	6.58	11.528	11.502	11.538	11.507	11.503
331	6.60	11.531	11.505	11.541	11.510	11.506
332	6.62	11.534	11.509	11.544	11.513	11.510
333	6.64	11.537	11.512	11.547	11.517	11.513
334	6.66	11.540	11.515	11.550	11.520	11.516
335	6.68	11.543	11.518	11.553	11.523	11.519
336	6.70	11.546	11.521	11.556	11.526	11.522
337	6.72	11.549	11.524	11.559	11.529	11.525
338	6.74	11.552	11.527	11.562	11.532	11.528
339	6.76	11.555	11.530	11.564	11.535	11.531
340	6.78	11.558	11.533	11.567	11.538	11.534
341	6.80	11.561	11.536	11.570	11.541	11.537
342	6.82	11.563	11.539	11.573	11.544	11.540
343	6.84	11.566	11.542	11.576	11.546	11.543
344	6.86	11.569	11.545	11.578	11.549	11.546
345	6.88	11.572	11.548	11.581	11.552	11.549
346	6.90	11.574	11.551	11.584	11.555	11.552
347	6.92	11.577	11.553	11.587	11.558	11.554
348	6.94	11.580	11.556	11.589	11.561	11.557
349	6.96	11.582	11.559	11.592	11.563	11.560
350	6.98	11.585	11.562	11.595	11.566	11.563
351	7.00	11.588	11.565	11.597	11.569	11.566

Appendix A. Supplementary Data

Table S2: Potentiometric Titration Data for the ML systems (M = Mg^{II}, Ca^{II}, Sr^{II}, and Ba^{II}; L = HIDS) in the Aqueous Matrix ($I = 0.1 \text{ mol}\cdot\text{dm}^{-3}$; $25 \pm 0.1^\circ\text{C}$; M:L = 1:1)

Sl	V _{KOH} /cm ³	HIDS	Mg ^{II} + HIDS	Ca ^{II} + HIDS	Sr ^{II} + HIDS	Ba ^{II} + HIDS
1	0.00	2.339	2.330	2.330	2.330	2.330
2	0.02	2.342	2.333	2.333	2.333	2.333
3	0.04	2.346	2.337	2.337	2.337	2.337
4	0.06	2.350	2.340	2.340	2.340	2.340
5	0.08	2.353	2.344	2.344	2.344	2.344
6	0.10	2.357	2.348	2.348	2.348	2.348
7	0.12	2.360	2.351	2.351	2.351	2.351
8	0.14	2.364	2.355	2.355	2.355	2.355
9	0.16	2.368	2.359	2.359	2.359	2.359
10	0.18	2.372	2.363	2.363	2.363	2.363
11	0.20	2.375	2.367	2.367	2.367	2.367
12	0.22	2.379	2.370	2.370	2.370	2.370
13	0.24	2.383	2.374	2.374	2.374	2.374
14	0.26	2.387	2.378	2.378	2.378	2.378
15	0.28	2.391	2.382	2.382	2.382	2.382
16	0.30	2.395	2.386	2.386	2.386	2.386
17	0.32	2.399	2.390	2.390	2.390	2.390
18	0.34	2.403	2.394	2.394	2.394	2.394
19	0.36	2.407	2.398	2.398	2.398	2.398
20	0.38	2.411	2.402	2.402	2.402	2.402
21	0.40	2.415	2.406	2.406	2.406	2.406
22	0.42	2.419	2.411	2.411	2.411	2.411
23	0.44	2.423	2.415	2.415	2.415	2.415
24	0.46	2.427	2.419	2.419	2.419	2.419
25	0.48	2.431	2.423	2.423	2.423	2.423
26	0.50	2.436	2.427	2.427	2.427	2.427
27	0.52	2.440	2.432	2.432	2.432	2.432
28	0.54	2.444	2.436	2.436	2.436	2.436
29	0.56	2.448	2.441	2.441	2.441	2.441
30	0.58	2.453	2.445	2.445	2.445	2.445
31	0.60	2.457	2.449	2.449	2.449	2.449
32	0.62	2.462	2.454	2.454	2.454	2.454
33	0.64	2.466	2.458	2.458	2.458	2.458
34	0.66	2.471	2.463	2.463	2.463	2.463
35	0.68	2.475	2.468	2.468	2.468	2.468
36	0.70	2.480	2.472	2.472	2.472	2.472
37	0.72	2.484	2.477	2.477	2.477	2.477
38	0.74	2.489	2.482	2.482	2.482	2.482
39	0.76	2.494	2.487	2.487	2.487	2.487
40	0.78	2.499	2.491	2.491	2.491	2.491
41	0.80	2.503	2.496	2.496	2.496	2.496
42	0.82	2.508	2.501	2.501	2.501	2.501

Appendix A. Supplementary Data

SI	$V_{\text{KOH}}/\text{cm}^3$	HIDS	$\text{Mg}^{\text{II}} + \text{HIDS}$	$\text{Ca}^{\text{II}} + \text{HIDS}$	$\text{Sr}^{\text{II}} + \text{HIDS}$	$\text{Ba}^{\text{II}} + \text{HIDS}$
43	0.84	2.513	2.506	2.506	2.506	2.506
44	0.86	2.518	2.511	2.511	2.511	2.511
45	0.88	2.523	2.516	2.516	2.516	2.516
46	0.90	2.528	2.521	2.521	2.521	2.521
47	0.92	2.533	2.526	2.526	2.526	2.526
48	0.94	2.538	2.532	2.532	2.532	2.532
49	0.96	2.543	2.537	2.537	2.537	2.537
50	0.98	2.549	2.542	2.542	2.542	2.542
51	1.00	2.554	2.547	2.547	2.547	2.547
52	1.02	2.559	2.553	2.553	2.553	2.553
53	1.04	2.565	2.558	2.558	2.558	2.558
54	1.06	2.570	2.564	2.564	2.564	2.564
55	1.08	2.576	2.569	2.569	2.569	2.569
56	1.10	2.581	2.575	2.575	2.575	2.575
57	1.12	2.587	2.581	2.581	2.581	2.581
58	1.14	2.592	2.586	2.586	2.586	2.586
59	1.16	2.598	2.592	2.592	2.592	2.592
60	1.18	2.604	2.598	2.598	2.598	2.598
61	1.20	2.610	2.604	2.604	2.604	2.604
62	1.22	2.616	2.610	2.610	2.610	2.610
63	1.24	2.622	2.616	2.616	2.616	2.616
64	1.26	2.628	2.622	2.622	2.622	2.622
65	1.28	2.634	2.628	2.628	2.628	2.628
66	1.30	2.640	2.635	2.635	2.635	2.635
67	1.32	2.646	2.641	2.641	2.641	2.641
68	1.34	2.653	2.647	2.647	2.647	2.647
69	1.36	2.659	2.654	2.654	2.654	2.654
70	1.38	2.666	2.661	2.661	2.661	2.661
71	1.40	2.672	2.667	2.667	2.667	2.667
72	1.42	2.679	2.674	2.674	2.674	2.674
73	1.44	2.686	2.681	2.681	2.681	2.681
74	1.46	2.692	2.688	2.688	2.688	2.688
75	1.48	2.699	2.695	2.695	2.695	2.695
76	1.50	2.706	2.702	2.702	2.702	2.702
77	1.52	2.713	2.709	2.709	2.709	2.709
78	1.54	2.721	2.716	2.716	2.716	2.716
79	1.56	2.728	2.723	2.723	2.723	2.723
80	1.58	2.735	2.731	2.731	2.731	2.731
81	1.60	2.743	2.738	2.738	2.738	2.738
82	1.62	2.750	2.746	2.746	2.746	2.746
83	1.64	2.758	2.754	2.754	2.754	2.754
84	1.66	2.766	2.762	2.762	2.762	2.762
85	1.68	2.773	2.770	2.770	2.770	2.770
86	1.70	2.781	2.778	2.778	2.778	2.778
87	1.72	2.790	2.786	2.786	2.786	2.786

Appendix A. Supplementary Data

SI	$V_{\text{KOH}}/\text{cm}^3$	HIDS	$\text{Mg}^{\text{II}} + \text{HIDS}$	$\text{Ca}^{\text{II}} + \text{HIDS}$	$\text{Sr}^{\text{II}} + \text{HIDS}$	$\text{Ba}^{\text{II}} + \text{HIDS}$
88	1.74	2.798	2.794	2.794	2.794	2.794
89	1.76	2.806	2.803	2.803	2.803	2.803
90	1.78	2.815	2.811	2.811	2.811	2.811
91	1.80	2.823	2.820	2.820	2.820	2.820
92	1.82	2.832	2.829	2.829	2.829	2.829
93	1.84	2.841	2.837	2.837	2.837	2.837
94	1.86	2.850	2.846	2.846	2.846	2.846
95	1.88	2.859	2.856	2.856	2.856	2.856
96	1.90	2.868	2.865	2.865	2.865	2.865
97	1.92	2.877	2.875	2.875	2.875	2.875
98	1.94	2.887	2.884	2.884	2.884	2.884
99	1.96	2.897	2.894	2.894	2.894	2.894
100	1.98	2.907	2.904	2.904	2.904	2.904
101	2.00	2.917	2.914	2.914	2.914	2.914
102	2.02	2.927	2.924	2.924	2.924	2.924
103	2.04	2.937	2.935	2.935	2.935	2.935
104	2.06	2.948	2.945	2.946	2.946	2.946
105	2.08	2.959	2.956	2.956	2.956	2.956
106	2.10	2.969	2.967	2.967	2.967	2.967
107	2.12	2.981	2.979	2.979	2.979	2.979
108	2.14	2.992	2.990	2.990	2.990	2.990
109	2.16	3.004	3.002	3.002	3.002	3.002
110	2.18	3.015	3.013	3.013	3.013	3.013
111	2.20	3.027	3.026	3.026	3.026	3.026
112	2.22	3.040	3.038	3.038	3.038	3.038
113	2.24	3.052	3.050	3.050	3.050	3.050
114	2.26	3.065	3.063	3.063	3.063	3.063
115	2.28	3.078	3.076	3.076	3.076	3.076
116	2.30	3.091	3.089	3.089	3.089	3.089
117	2.32	3.104	3.103	3.103	3.103	3.103
118	2.34	3.118	3.117	3.117	3.117	3.117
119	2.36	3.132	3.131	3.131	3.131	3.131
120	2.38	3.146	3.145	3.145	3.145	3.145
121	2.40	3.161	3.160	3.160	3.160	3.160
122	2.42	3.176	3.175	3.175	3.175	3.175
123	2.44	3.191	3.190	3.190	3.190	3.190
124	2.46	3.207	3.206	3.206	3.206	3.206
125	2.48	3.223	3.222	3.222	3.222	3.222
126	2.50	3.239	3.238	3.238	3.238	3.238
127	2.52	3.256	3.255	3.255	3.255	3.255
128	2.54	3.273	3.272	3.272	3.272	3.272
129	2.56	3.290	3.290	3.290	3.290	3.290
130	2.58	3.308	3.308	3.308	3.308	3.308
131	2.60	3.327	3.326	3.326	3.326	3.326
132	2.62	3.345	3.345	3.345	3.345	3.345

Appendix A. Supplementary Data

SI	$V_{\text{KOH}}/\text{cm}^3$	HIDS	$\text{Mg}^{\text{II}} + \text{HIDS}$	$\text{Ca}^{\text{II}} + \text{HIDS}$	$\text{Sr}^{\text{II}} + \text{HIDS}$	$\text{Ba}^{\text{II}} + \text{HIDS}$
133	2.64	3.365	3.364	3.364	3.364	3.364
134	2.66	3.384	3.384	3.384	3.384	3.384
135	2.68	3.404	3.404	3.404	3.404	3.404
136	2.70	3.425	3.425	3.425	3.425	3.425
137	2.72	3.446	3.446	3.446	3.446	3.446
138	2.74	3.468	3.468	3.468	3.468	3.468
139	2.76	3.490	3.490	3.490	3.490	3.490
140	2.78	3.513	3.513	3.513	3.513	3.513
141	2.80	3.536	3.536	3.536	3.536	3.536
142	2.82	3.560	3.560	3.560	3.560	3.560
143	2.84	3.585	3.585	3.585	3.585	3.585
144	2.86	3.610	3.610	3.610	3.610	3.610
145	2.88	3.636	3.636	3.636	3.636	3.636
146	2.90	3.663	3.662	3.663	3.663	3.663
147	2.92	3.690	3.690	3.690	3.690	3.690
148	2.94	3.718	3.718	3.718	3.718	3.718
149	2.96	3.747	3.747	3.747	3.747	3.747
150	2.98	3.776	3.776	3.776	3.776	3.776
151	3.00	3.807	3.807	3.807	3.807	3.807
152	3.02	3.838	3.838	3.838	3.838	3.838
153	3.04	3.870	3.870	3.870	3.870	3.870
154	3.06	3.903	3.903	3.903	3.903	3.903
155	3.08	3.938	3.937	3.937	3.938	3.938
156	3.10	3.973	3.972	3.973	3.973	3.973
157	3.12	4.009	4.009	4.009	4.009	4.009
158	3.14	4.047	4.046	4.047	4.047	4.047
159	3.16	4.086	4.085	4.086	4.086	4.086
160	3.18	4.127	4.126	4.127	4.127	4.127
161	3.20	4.169	4.168	4.169	4.169	4.169
162	3.22	4.214	4.213	4.214	4.214	4.214
163	3.24	4.261	4.259	4.260	4.261	4.261
164	3.26	4.310	4.308	4.310	4.310	4.310
165	3.28	4.363	4.361	4.362	4.363	4.363
166	3.30	4.420	4.417	4.419	4.419	4.419
167	3.32	4.481	4.477	4.480	4.480	4.481
168	3.34	4.548	4.543	4.546	4.547	4.548
169	3.36	4.623	4.616	4.621	4.622	4.623
170	3.38	4.708	4.698	4.705	4.706	4.708
171	3.40	4.807	4.793	4.803	4.805	4.807
172	3.42	4.928	4.906	4.921	4.925	4.928
173	3.44	5.086	5.045	5.072	5.080	5.086
174	3.46	5.320	5.225	5.284	5.304	5.318
175	3.48	5.805	5.463	5.619	5.700	5.786
176	3.50	7.884	5.742	6.089	6.375	7.096
177	3.52	8.373	5.997	6.445	6.795	7.582

Appendix A. Supplementary Data

SI	$V_{\text{KOH}}/\text{cm}^3$	HIDS	$\text{Mg}^{\text{II}} + \text{HIDS}$	$\text{Ca}^{\text{II}} + \text{HIDS}$	$\text{Sr}^{\text{II}} + \text{HIDS}$	$\text{Ba}^{\text{II}} + \text{HIDS}$
178	3.54	8.610	6.201	6.681	7.044	7.832
179	3.56	8.773	6.367	6.859	7.227	8.007
180	3.58	8.898	6.509	7.006	7.376	8.147
181	3.60	9.003	6.635	7.134	7.505	8.266
182	3.62	9.093	6.750	7.250	7.622	8.370
183	3.64	9.174	6.859	7.358	7.731	8.465
184	3.66	9.247	6.963	7.461	7.834	8.552
185	3.68	9.315	7.064	7.561	7.934	8.634
186	3.70	9.379	7.165	7.660	8.031	8.712
187	3.72	9.439	7.265	7.758	8.127	8.786
188	3.74	9.497	7.367	7.857	8.223	8.858
189	3.76	9.553	7.471	7.957	8.318	8.926
190	3.78	9.606	7.579	8.060	8.414	8.993
191	3.80	9.659	7.692	8.167	8.510	9.058
192	3.82	9.710	7.812	8.278	8.607	9.121
193	3.84	9.760	7.940	8.395	8.703	9.183
194	3.86	9.809	8.079	8.518	8.799	9.243
195	3.88	9.857	8.230	8.649	8.893	9.301
196	3.90	9.904	8.396	8.787	8.985	9.359
197	3.92	9.951	8.578	8.930	9.074	9.414
198	3.94	9.996	8.772	9.077	9.159	9.468
199	3.96	10.040	8.968	9.222	9.241	9.521
200	3.98	10.083	9.153	9.361	9.318	9.573
201	4.00	10.125	9.315	9.489	9.390	9.622
202	4.02	10.165	9.454	9.604	9.459	9.671
203	4.04	10.204	9.572	9.705	9.523	9.718
204	4.06	10.242	9.672	9.794	9.584	9.763
205	4.08	10.278	9.758	9.873	9.642	9.807
206	4.10	10.313	9.834	9.942	9.697	9.850
207	4.12	10.346	9.900	10.005	9.748	9.891
208	4.14	10.378	9.960	10.061	9.798	9.931
209	4.16	10.408	10.014	10.111	9.845	9.970
210	4.18	10.437	10.063	10.158	9.890	10.007
211	4.20	10.465	10.109	10.200	9.933	10.044
212	4.22	10.492	10.151	10.240	9.974	10.079
213	4.24	10.517	10.190	10.276	10.013	10.113
214	4.26	10.542	10.226	10.311	10.051	10.145
215	4.28	10.565	10.260	10.343	10.088	10.177
216	4.30	10.588	10.293	10.373	10.123	10.208
217	4.32	10.609	10.323	10.401	10.157	10.238
218	4.34	10.630	10.352	10.428	10.190	10.267
219	4.36	10.650	10.380	10.454	10.222	10.295
220	4.38	10.669	10.406	10.478	10.252	10.322
221	4.40	10.687	10.431	10.502	10.282	10.348
222	4.42	10.705	10.455	10.524	10.311	10.373

Appendix A. Supplementary Data

SI	$V_{\text{KOH}}/\text{cm}^3$	HIDS	$\text{Mg}^{\text{II}} + \text{HIDS}$	$\text{Ca}^{\text{II}} + \text{HIDS}$	$\text{Sr}^{\text{II}} + \text{HIDS}$	$\text{Ba}^{\text{II}} + \text{HIDS}$
223	4.44	10.722	10.478	10.545	10.338	10.398
224	4.46	10.739	10.500	10.566	10.365	10.422
225	4.48	10.755	10.521	10.586	10.391	10.445
226	4.50	10.770	10.542	10.605	10.416	10.467
227	4.52	10.785	10.562	10.623	10.441	10.489
228	4.54	10.800	10.581	10.640	10.464	10.510
229	4.56	10.814	10.599	10.657	10.487	10.531
230	4.58	10.828	10.617	10.674	10.509	10.551
231	4.60	10.841	10.634	10.690	10.530	10.570
232	4.62	10.854	10.651	10.705	10.551	10.589
233	4.64	10.866	10.668	10.720	10.571	10.607
234	4.66	10.879	10.683	10.735	10.591	10.625
235	4.68	10.891	10.699	10.749	10.610	10.643
236	4.70	10.902	10.714	10.763	10.628	10.659
237	4.72	10.914	10.728	10.776	10.646	10.676
238	4.74	10.925	10.743	10.789	10.664	10.692
239	4.76	10.935	10.756	10.802	10.680	10.707
240	4.78	10.946	10.770	10.815	10.697	10.722
241	4.80	10.956	10.783	10.827	10.713	10.737
242	4.82	10.966	10.796	10.839	10.728	10.751
243	4.84	10.976	10.808	10.850	10.743	10.765
244	4.86	10.986	10.821	10.861	10.758	10.779
245	4.88	10.995	10.832	10.872	10.772	10.792
246	4.90	11.004	10.844	10.883	10.786	10.805
247	4.92	11.013	10.856	10.894	10.800	10.818
248	4.94	11.022	10.867	10.904	10.813	10.831
249	4.96	11.031	10.878	10.914	10.826	10.843
250	4.98	11.039	10.888	10.924	10.838	10.854
251	5.00	11.047	10.899	10.934	10.851	10.866
252	5.02	11.056	10.909	10.943	10.863	10.877
253	5.04	11.064	10.919	10.953	10.874	10.889
254	5.06	11.071	10.929	10.962	10.886	10.899
255	5.08	11.079	10.939	10.971	10.897	10.910
256	5.10	11.087	10.948	10.980	10.908	10.920
257	5.12	11.094	10.958	10.988	10.919	10.931
258	5.14	11.101	10.967	10.997	10.929	10.941
259	5.16	11.109	10.976	11.005	10.940	10.950
260	5.18	11.116	10.985	11.014	10.950	10.960
261	5.20	11.123	10.993	11.022	10.959	10.969
262	5.22	11.130	11.002	11.030	10.969	10.979
263	5.24	11.136	11.010	11.037	10.979	10.988
264	5.26	11.143	11.019	11.045	10.988	10.997
265	5.28	11.149	11.027	11.053	10.997	11.005
266	5.30	11.156	11.035	11.060	11.006	11.014
267	5.32	11.162	11.042	11.067	11.015	11.022

Appendix A. Supplementary Data

SI	$V_{\text{KOH}}/\text{cm}^3$	HIDS	$\text{Mg}^{\text{II}} + \text{HIDS}$	$\text{Ca}^{\text{II}} + \text{HIDS}$	$\text{Sr}^{\text{II}} + \text{HIDS}$	$\text{Ba}^{\text{II}} + \text{HIDS}$
268	5.34	11.168	11.050	11.075	11.023	11.031
269	5.36	11.175	11.058	11.082	11.032	11.039
270	5.38	11.181	11.065	11.089	11.040	11.047
271	5.40	11.187	11.073	11.096	11.048	11.055
272	5.42	11.193	11.080	11.103	11.056	11.062
273	5.44	11.198	11.087	11.109	11.064	11.070
274	5.46	11.204	11.094	11.116	11.072	11.077
275	5.48	11.210	11.101	11.122	11.079	11.085
276	5.50	11.215	11.108	11.129	11.087	11.092
277	5.52	11.221	11.114	11.135	11.094	11.099
278	5.54	11.226	11.121	11.141	11.101	11.106
279	5.56	11.232	11.128	11.148	11.108	11.113
280	5.58	11.237	11.134	11.154	11.115	11.120
281	5.60	11.242	11.140	11.160	11.122	11.127
282	5.62	11.247	11.147	11.166	11.129	11.133
283	5.64	11.252	11.153	11.171	11.136	11.140
284	5.66	11.257	11.159	11.177	11.142	11.146
285	5.68	11.262	11.165	11.183	11.149	11.153
286	5.70	11.267	11.171	11.189	11.155	11.159
287	5.72	11.272	11.177	11.194	11.161	11.165
288	5.74	11.277	11.183	11.200	11.168	11.171
289	5.76	11.282	11.188	11.205	11.174	11.177
290	5.78	11.287	11.194	11.211	11.180	11.183
291	5.80	11.291	11.200	11.216	11.186	11.189
292	5.82	11.296	11.205	11.221	11.192	11.195
293	5.84	11.300	11.211	11.226	11.197	11.200
294	5.86	11.305	11.216	11.231	11.203	11.206
295	5.88	11.309	11.221	11.236	11.209	11.211
296	5.90	11.314	11.227	11.241	11.214	11.217
297	5.92	11.318	11.232	11.246	11.220	11.222
298	5.94	11.322	11.237	11.251	11.225	11.228
299	5.96	11.327	11.242	11.256	11.231	11.233
300	5.98	11.331	11.247	11.261	11.236	11.238
301	6.00	11.335	11.252	11.266	11.241	11.243
302	6.02	11.339	11.257	11.270	11.246	11.248
303	6.04	11.343	11.262	11.275	11.252	11.253
304	6.06	11.347	11.267	11.280	11.257	11.258
305	6.08	11.351	11.271	11.284	11.262	11.263
306	6.10	11.355	11.276	11.289	11.267	11.268
307	6.12	11.359	11.281	11.293	11.271	11.273
308	6.14	11.363	11.285	11.298	11.276	11.278
309	6.16	11.367	11.290	11.302	11.281	11.282
310	6.18	11.371	11.294	11.306	11.286	11.287
311	6.20	11.374	11.299	11.311	11.290	11.292
312	6.22	11.378	11.303	11.315	11.295	11.296

Appendix A. Supplementary Data

Sl	$V_{\text{KOH}}/\text{cm}^3$	HIDS	$\text{Mg}^{\text{II}} + \text{HIDS}$	$\text{Ca}^{\text{II}} + \text{HIDS}$	$\text{Sr}^{\text{II}} + \text{HIDS}$	$\text{Ba}^{\text{II}} + \text{HIDS}$
313	6.24	11.382	11.308	11.319	11.300	11.301
314	6.26	11.386	11.312	11.323	11.304	11.305
315	6.28	11.389	11.316	11.327	11.309	11.310
316	6.30	11.393	11.320	11.331	11.313	11.314
317	6.32	11.396	11.325	11.335	11.317	11.318
318	6.34	11.400	11.329	11.339	11.322	11.322
319	6.36	11.403	11.333	11.343	11.326	11.327
320	6.38	11.407	11.337	11.347	11.330	11.331
321	6.40	11.410	11.341	11.351	11.334	11.335
322	6.42	11.414	11.345	11.355	11.338	11.339
323	6.44	11.417	11.349	11.359	11.343	11.343
324	6.46	11.421	11.353	11.363	11.347	11.347
325	6.48	11.424	11.357	11.367	11.351	11.351
326	6.50	11.427	11.361	11.370	11.355	11.355
327	6.52	11.431	11.364	11.374	11.359	11.359
328	6.54	11.434	11.368	11.378	11.363	11.363
329	6.56	11.437	11.372	11.381	11.366	11.367
330	6.58	11.440	11.376	11.385	11.370	11.371
331	6.60	11.443	11.379	11.388	11.374	11.374
332	6.62	11.447	11.383	11.392	11.378	11.378
333	6.64	11.450	11.387	11.395	11.382	11.382
334	6.66	11.453	11.390	11.399	11.385	11.386
335	6.68	11.456	11.394	11.402	11.389	11.389
336	6.70	11.459	11.397	11.406	11.393	11.393
337	6.72	11.462	11.401	11.409	11.396	11.396
338	6.74	11.465	11.404	11.413	11.400	11.400
339	6.76	11.468	11.408	11.416	11.403	11.403
340	6.78	11.471	11.411	11.419	11.407	11.407
341	6.80	11.474	11.415	11.423	11.410	11.410
342	6.82	11.477	11.418	11.426	11.414	11.414
343	6.84	11.480	11.421	11.429	11.417	11.417
344	6.86	11.483	11.425	11.432	11.421	11.421
345	6.88	11.485	11.428	11.436	11.424	11.424
346	6.90	11.488	11.431	11.439	11.427	11.427
347	6.92	11.491	11.434	11.442	11.431	11.431
348	6.94	11.494	11.438	11.445	11.434	11.434
349	6.96	11.497	11.441	11.448	11.437	11.437
350	6.98	11.499	11.444	11.451	11.441	11.440
351	7.00	11.502	11.447	11.454	11.444	11.444

Appendix A. Supplementary Data

Table S3: Potentiometric Titration Data for the ML systems (M = Y^{II}; L = GLDA and HIDS) in the Aqueous Matrix ($I = 0.1 \text{ mol} \cdot \text{dm}^{-3}$; $25 \pm 0.1^\circ\text{C}$; M:L = 1:1)

Sl	V _{KOH} /cm ³	GLDA	Y ^{III} + GLDA	HIDS	Y ^{III} + HIDS
1	0.00	2.243	2.171	2.339	2.240
2	0.02	2.247	2.173	2.342	2.242
3	0.04	2.250	2.176	2.346	2.245
4	0.06	2.254	2.178	2.350	2.248
5	0.08	2.257	2.181	2.353	2.250
6	0.10	2.261	2.183	2.357	2.253
7	0.12	2.265	2.186	2.360	2.256
8	0.14	2.269	2.188	2.364	2.258
9	0.16	2.272	2.191	2.368	2.261
10	0.18	2.276	2.193	2.372	2.264
11	0.20	2.280	2.196	2.375	2.266
12	0.22	2.284	2.198	2.379	2.269
13	0.24	2.288	2.201	2.383	2.272
14	0.26	2.292	2.204	2.387	2.275
15	0.28	2.296	2.206	2.391	2.277
16	0.30	2.299	2.209	2.395	2.280
17	0.32	2.303	2.211	2.399	2.283
18	0.34	2.308	2.214	2.403	2.286
19	0.36	2.312	2.217	2.407	2.289
20	0.38	2.316	2.219	2.411	2.291
21	0.40	2.320	2.222	2.415	2.294
22	0.42	2.324	2.225	2.419	2.297
23	0.44	2.328	2.227	2.423	2.300
24	0.46	2.332	2.230	2.427	2.303
25	0.48	2.337	2.233	2.431	2.306
26	0.50	2.341	2.235	2.436	2.309
27	0.52	2.345	2.238	2.440	2.312
28	0.54	2.350	2.241	2.444	2.315
29	0.56	2.354	2.244	2.448	2.318
30	0.58	2.359	2.246	2.453	2.321
31	0.60	2.363	2.249	2.457	2.324
32	0.62	2.368	2.252	2.462	2.327
33	0.64	2.372	2.255	2.466	2.330
34	0.66	2.377	2.258	2.471	2.333
35	0.68	2.381	2.260	2.475	2.336
36	0.70	2.386	2.263	2.480	2.339
37	0.72	2.391	2.266	2.484	2.342
38	0.74	2.396	2.269	2.489	2.345
39	0.76	2.400	2.272	2.494	2.348
40	0.78	2.405	2.275	2.499	2.351
41	0.80	2.410	2.278	2.503	2.355
42	0.82	2.415	2.281	2.508	2.358

Appendix A. Supplementary Data

SI	$V_{\text{KOH}}/\text{cm}^3$	GLDA	$Y^{\text{III}} + \text{GLDA}$	HIDS	$Y^{\text{III}} + \text{HIDS}$
43	0.84	2.420	2.283	2.513	2.361
44	0.86	2.425	2.286	2.518	2.364
45	0.88	2.430	2.289	2.523	2.368
46	0.90	2.435	2.292	2.528	2.371
47	0.92	2.441	2.295	2.533	2.374
48	0.94	2.446	2.298	2.538	2.377
49	0.96	2.451	2.301	2.543	2.381
50	0.98	2.457	2.304	2.549	2.384
51	1.00	2.462	2.308	2.554	2.387
52	1.02	2.468	2.311	2.559	2.391
53	1.04	2.473	2.314	2.565	2.394
54	1.06	2.479	2.317	2.570	2.398
55	1.08	2.484	2.320	2.576	2.401
56	1.10	2.490	2.323	2.581	2.405
57	1.12	2.496	2.326	2.587	2.408
58	1.14	2.502	2.329	2.592	2.412
59	1.16	2.508	2.333	2.598	2.415
60	1.18	2.514	2.336	2.604	2.419
61	1.20	2.520	2.339	2.610	2.422
62	1.22	2.526	2.342	2.616	2.426
63	1.24	2.532	2.346	2.622	2.430
64	1.26	2.538	2.349	2.628	2.433
65	1.28	2.545	2.352	2.634	2.437
66	1.30	2.551	2.356	2.640	2.441
67	1.32	2.558	2.359	2.646	2.445
68	1.34	2.564	2.362	2.653	2.448
69	1.36	2.571	2.366	2.659	2.452
70	1.38	2.578	2.369	2.666	2.456
71	1.40	2.585	2.373	2.672	2.460
72	1.42	2.592	2.376	2.679	2.464
73	1.44	2.599	2.380	2.686	2.468
74	1.46	2.606	2.383	2.692	2.472
75	1.48	2.613	2.387	2.699	2.476
76	1.50	2.620	2.391	2.706	2.480
77	1.52	2.628	2.394	2.713	2.484
78	1.54	2.635	2.398	2.721	2.488
79	1.56	2.643	2.401	2.728	2.492
80	1.58	2.651	2.405	2.735	2.496
81	1.60	2.659	2.409	2.743	2.500
82	1.62	2.666	2.413	2.750	2.504
83	1.64	2.675	2.416	2.758	2.509
84	1.66	2.683	2.420	2.766	2.513
85	1.68	2.691	2.424	2.773	2.517
86	1.70	2.700	2.428	2.781	2.522
87	1.72	2.708	2.432	2.790	2.526

Appendix A. Supplementary Data

SI	$V_{\text{KOH}}/\text{cm}^3$	GLDA	$Y^{\text{III}} + \text{GLDA}$	HIDS	$Y^{\text{III}} + \text{HIDS}$
88	1.74	2.717	2.436	2.798	2.530
89	1.76	2.726	2.440	2.806	2.535
90	1.78	2.735	2.444	2.815	2.539
91	1.80	2.744	2.448	2.823	2.544
92	1.82	2.753	2.452	2.832	2.548
93	1.84	2.763	2.456	2.841	2.553
94	1.86	2.773	2.460	2.850	2.558
95	1.88	2.782	2.464	2.859	2.562
96	1.90	2.792	2.469	2.868	2.567
97	1.92	2.803	2.473	2.877	2.572
98	1.94	2.813	2.477	2.887	2.577
99	1.96	2.824	2.482	2.897	2.581
100	1.98	2.834	2.486	2.907	2.586
101	2.00	2.845	2.490	2.917	2.591
102	2.02	2.857	2.495	2.927	2.596
103	2.04	2.868	2.499	2.937	2.601
104	2.06	2.880	2.504	2.948	2.606
105	2.08	2.892	2.509	2.959	2.612
106	2.10	2.904	2.513	2.969	2.617
107	2.12	2.916	2.518	2.981	2.622
108	2.14	2.929	2.523	2.992	2.627
109	2.16	2.942	2.528	3.004	2.633
110	2.18	2.955	2.533	3.015	2.638
111	2.20	2.968	2.537	3.027	2.643
112	2.22	2.982	2.542	3.040	2.649
113	2.24	2.996	2.548	3.052	2.654
114	2.26	3.011	2.553	3.065	2.660
115	2.28	3.026	2.558	3.078	2.666
116	2.30	3.041	2.563	3.091	2.671
117	2.32	3.057	2.568	3.104	2.677
118	2.34	3.072	2.574	3.118	2.683
119	2.36	3.089	2.579	3.132	2.689
120	2.38	3.106	2.585	3.146	2.695
121	2.40	3.123	2.590	3.161	2.701
122	2.42	3.141	2.596	3.176	2.707
123	2.44	3.159	2.602	3.191	2.713
124	2.46	3.178	2.608	3.207	2.720
125	2.48	3.197	2.613	3.223	2.726
126	2.50	3.217	2.619	3.239	2.732
127	2.52	3.237	2.625	3.256	2.739
128	2.54	3.258	2.632	3.273	2.745
129	2.56	3.280	2.638	3.290	2.752
130	2.58	3.303	2.644	3.308	2.759
131	2.60	3.326	2.651	3.327	2.765
132	2.62	3.350	2.657	3.345	2.772

Appendix A. Supplementary Data

SI	$V_{\text{KOH}}/\text{cm}^3$	GLDA	$Y^{\text{III}} + \text{GLDA}$	HIDS	$Y^{\text{III}} + \text{HIDS}$
133	2.64	3.375	2.664	3.365	2.779
134	2.66	3.400	2.671	3.384	2.786
135	2.68	3.427	2.677	3.404	2.793
136	2.70	3.455	2.684	3.425	2.800
137	2.72	3.483	2.692	3.446	2.808
138	2.74	3.513	2.699	3.468	2.815
139	2.76	3.544	2.706	3.490	2.823
140	2.78	3.577	2.714	3.513	2.830
141	2.80	3.610	2.721	3.536	2.838
142	2.82	3.646	2.729	3.560	2.846
143	2.84	3.683	2.737	3.585	2.854
144	2.86	3.722	2.745	3.610	2.862
145	2.88	3.762	2.753	3.636	2.870
146	2.90	3.805	2.762	3.663	2.878
147	2.92	3.851	2.770	3.690	2.886
148	2.94	3.899	2.779	3.718	2.895
149	2.96	3.949	2.788	3.747	2.903
150	2.98	4.003	2.797	3.776	2.912
151	3.00	4.059	2.807	3.807	2.920
152	3.02	4.119	2.816	3.838	2.929
153	3.04	4.182	2.826	3.870	2.938
154	3.06	4.248	2.836	3.903	2.948
155	3.08	4.316	2.846	3.938	2.957
156	3.10	4.386	2.857	3.973	2.966
157	3.12	4.458	2.868	4.009	2.976
158	3.14	4.531	2.879	4.047	2.986
159	3.16	4.604	2.890	4.086	2.996
160	3.18	4.678	2.902	4.127	3.006
161	3.20	4.752	2.914	4.169	3.016
162	3.22	4.826	2.927	4.214	3.026
163	3.24	4.900	2.940	4.261	3.037
164	3.26	4.976	2.953	4.310	3.047
165	3.28	5.053	2.967	4.363	3.058
166	3.30	5.132	2.981	4.420	3.069
167	3.32	5.216	2.996	4.481	3.080
168	3.34	5.305	3.011	4.548	3.092
169	3.36	5.402	3.027	4.623	3.103
170	3.38	5.510	3.043	4.708	3.115
171	3.40	5.637	3.060	4.807	3.127
172	3.42	5.793	3.078	4.928	3.139
173	3.44	6.007	3.097	5.086	3.151
174	3.46	6.372	3.116	5.320	3.164
175	3.48	7.507	3.137	5.805	3.177
176	3.50	8.192	3.158	7.884	3.190
177	3.52	8.473	3.180	8.373	3.203

Appendix A. Supplementary Data

SI	$V_{\text{KOH}}/\text{cm}^3$	GLDA	$Y^{\text{III}} + \text{GLDA}$	HIDS	$Y^{\text{III}} + \text{HIDS}$
178	3.54	8.658	3.204	8.610	3.217
179	3.56	8.800	3.229	8.773	3.231
180	3.58	8.918	3.255	8.898	3.245
181	3.60	9.021	3.283	9.003	3.259
182	3.62	9.114	3.312	9.093	3.274
183	3.64	9.199	3.344	9.174	3.289
184	3.66	9.280	3.377	9.247	3.304
185	3.68	9.358	3.413	9.315	3.320
186	3.70	9.433	3.451	9.379	3.336
187	3.72	9.506	3.492	9.439	3.352
188	3.74	9.578	3.535	9.497	3.369
189	3.76	9.649	3.582	9.553	3.386
190	3.78	9.719	3.632	9.606	3.403
191	3.80	9.788	3.685	9.659	3.421
192	3.82	9.857	3.741	9.710	3.440
193	3.84	9.923	3.800	9.760	3.459
194	3.86	9.988	3.862	9.809	3.478
195	3.88	10.050	3.926	9.857	3.498
196	3.90	10.109	3.991	9.904	3.518
197	3.92	10.165	4.058	9.951	3.540
198	3.94	10.217	4.126	9.996	3.561
199	3.96	10.266	4.196	10.040	3.584
200	3.98	10.312	4.267	10.083	3.607
201	4.00	10.355	4.339	10.125	3.632
202	4.02	10.396	4.413	10.165	3.657
203	4.04	10.433	4.490	10.204	3.683
204	4.06	10.468	4.570	10.242	3.710
205	4.08	10.501	4.656	10.278	3.738
206	4.10	10.532	4.748	10.313	3.768
207	4.12	10.562	4.851	10.346	3.799
208	4.14	10.589	4.968	10.378	3.832
209	4.16	10.616	5.107	10.408	3.867
210	4.18	10.640	5.287	10.437	3.903
211	4.20	10.664	5.553	10.465	3.943
212	4.22	10.687	6.167	10.492	3.985
213	4.24	10.708	9.049	10.517	4.030
214	4.26	10.729	9.497	10.542	4.079
215	4.28	10.748	9.727	10.565	4.133
216	4.30	10.767	9.880	10.588	4.193
217	4.32	10.785	9.995	10.609	4.260
218	4.34	10.802	10.086	10.630	4.336
219	4.36	10.819	10.162	10.650	4.425
220	4.38	10.835	10.226	10.669	4.532
221	4.40	10.851	10.283	10.687	4.666
222	4.42	10.866	10.333	10.705	4.838

Appendix A. Supplementary Data

SI	$V_{\text{KOH}}/\text{cm}^3$	GLDA	$Y^{\text{III}} + \text{GLDA}$	HIDS	$Y^{\text{III}} + \text{HIDS}$
223	4.44	10.881	10.377	10.722	5.064
224	4.46	10.895	10.418	10.739	5.323
225	4.48	10.908	10.455	10.755	5.556
226	4.50	10.922	10.490	10.770	5.740
227	4.52	10.934	10.521	10.785	5.887
228	4.54	10.947	10.551	10.800	6.008
229	4.56	10.959	10.579	10.814	6.113
230	4.58	10.971	10.605	10.828	6.207
231	4.60	10.982	10.629	10.841	6.293
232	4.62	10.993	10.652	10.854	6.373
233	4.64	11.004	10.675	10.866	6.449
234	4.66	11.015	10.696	10.879	6.523
235	4.68	11.025	10.716	10.891	6.595
236	4.70	11.036	10.735	10.902	6.667
237	4.72	11.045	10.753	10.914	6.740
238	4.74	11.055	10.771	10.925	6.814
239	4.76	11.065	10.787	10.935	6.891
240	4.78	11.074	10.804	10.946	6.972
241	4.80	11.083	10.819	10.956	7.059
242	4.82	11.092	10.835	10.966	7.154
243	4.84	11.100	10.849	10.976	7.263
244	4.86	11.109	10.863	10.986	7.391
245	4.88	11.117	10.877	10.995	7.551
246	4.90	11.126	10.890	11.004	7.769
247	4.92	11.134	10.903	11.013	8.109
248	4.94	11.141	10.916	11.022	8.572
249	4.96	11.149	10.928	11.031	8.908
250	4.98	11.157	10.939	11.039	9.121
251	5.00	11.164	10.951	11.047	9.274
252	5.02	11.172	10.962	11.056	9.394
253	5.04	11.179	10.973	11.064	9.492
254	5.06	11.186	10.984	11.071	9.576
255	5.08	11.193	10.994	11.079	9.650
256	5.10	11.200	11.004	11.087	9.716
257	5.12	11.207	11.014	11.094	9.776
258	5.14	11.213	11.024	11.101	9.831
259	5.16	11.220	11.033	11.109	9.882
260	5.18	11.226	11.042	11.116	9.929
261	5.20	11.232	11.051	11.123	9.973
262	5.22	11.239	11.060	11.130	10.015
263	5.24	11.245	11.069	11.136	10.055
264	5.26	11.251	11.078	11.143	10.092
265	5.28	11.257	11.086	11.149	10.128
266	5.30	11.263	11.094	11.156	10.162
267	5.32	11.269	11.102	11.162	10.195

Appendix A. Supplementary Data

SI	$V_{\text{KOH}}/\text{cm}^3$	GLDA	$Y^{\text{III}} + \text{GLDA}$	HIDS	$Y^{\text{III}} + \text{HIDS}$
268	5.34	11.274	11.110	11.168	10.226
269	5.36	11.280	11.118	11.175	10.256
270	5.38	11.286	11.125	11.181	10.285
271	5.40	11.291	11.133	11.187	10.313
272	5.42	11.296	11.140	11.193	10.339
273	5.44	11.302	11.147	11.198	10.365
274	5.46	11.307	11.154	11.204	10.390
275	5.48	11.312	11.161	11.210	10.414
276	5.50	11.317	11.168	11.215	10.438
277	5.52	11.323	11.175	11.221	10.460
278	5.54	11.328	11.182	11.226	10.482
279	5.56	11.333	11.188	11.232	10.503
280	5.58	11.337	11.195	11.237	10.524
281	5.60	11.342	11.201	11.242	10.543
282	5.62	11.347	11.207	11.247	10.563
283	5.64	11.352	11.213	11.252	10.581
284	5.66	11.357	11.220	11.257	10.600
285	5.68	11.361	11.225	11.262	10.617
286	5.70	11.366	11.231	11.267	10.634
287	5.72	11.370	11.237	11.272	10.651
288	5.74	11.375	11.243	11.277	10.667
289	5.76	11.379	11.249	11.282	10.683
290	5.78	11.384	11.254	11.287	10.698
291	5.80	11.388	11.260	11.291	10.713
292	5.82	11.392	11.265	11.296	10.728
293	5.84	11.396	11.271	11.300	10.742
294	5.86	11.401	11.276	11.305	10.756
295	5.88	11.405	11.281	11.309	10.769
296	5.90	11.409	11.286	11.314	10.782
297	5.92	11.413	11.291	11.318	10.795
298	5.94	11.417	11.296	11.322	10.807
299	5.96	11.421	11.301	11.327	10.820
300	5.98	11.425	11.306	11.331	10.832
301	6.00	11.429	11.311	11.335	10.843
302	6.02	11.433	11.316	11.339	10.855
303	6.04	11.437	11.321	11.343	10.866
304	6.06	11.440	11.326	11.347	10.877
305	6.08	11.444	11.330	11.351	10.887
306	6.10	11.448	11.335	11.355	10.898
307	6.12	11.452	11.339	11.359	10.908
308	6.14	11.455	11.344	11.363	10.918
309	6.16	11.459	11.348	11.367	10.928
310	6.18	11.463	11.353	11.371	10.938
311	6.20	11.466	11.357	11.374	10.947
312	6.22	11.470	11.361	11.378	10.956

Appendix A. Supplementary Data

Sl	$V_{\text{KOH}}/\text{cm}^3$	GLDA	$Y^{\text{III}} + \text{GLDA}$	HIDS	$Y^{\text{III}} + \text{HIDS}$
313	6.24	11.473	11.366	11.382	10.965
314	6.26	11.477	11.370	11.386	10.974
315	6.28	11.480	11.374	11.389	10.983
316	6.30	11.483	11.378	11.393	10.992
317	6.32	11.487	11.382	11.396	11.000
318	6.34	11.490	11.386	11.400	11.008
319	6.36	11.494	11.390	11.403	11.016
320	6.38	11.497	11.394	11.407	11.024
321	6.40	11.500	11.398	11.410	11.032
322	6.42	11.503	11.402	11.414	11.040
323	6.44	11.507	11.406	11.417	11.048
324	6.46	11.510	11.410	11.421	11.055
325	6.48	11.513	11.414	11.424	11.063
326	6.50	11.516	11.417	11.427	11.070
327	6.52	11.519	11.421	11.431	11.077
328	6.54	11.522	11.425	11.434	11.084
329	6.56	11.525	11.429	11.437	11.091
330	6.58	11.528	11.432	11.440	11.098
331	6.60	11.531	11.436	11.443	11.104
332	6.62	11.534	11.439	11.447	11.111
333	6.64	11.537	11.443	11.450	11.117
334	6.66	11.540	11.446	11.453	11.124
335	6.68	11.543	11.450	11.456	11.130
336	6.70	11.546	11.453	11.459	11.136
337	6.72	11.549	11.457	11.462	11.143
338	6.74	11.552	11.460	11.465	11.149
339	6.76	11.555	11.464	11.468	11.155
340	6.78	11.558	11.467	11.471	11.161
341	6.80	11.561	11.470	11.474	11.166
342	6.82	11.563	11.473	11.477	11.172
343	6.84	11.566	11.477	11.480	11.178
344	6.86	11.569	11.480	11.483	11.183
345	6.88	11.572	11.483	11.485	11.189
346	6.90	11.574	11.486	11.488	11.194
347	6.92	11.577	11.489	11.491	11.200
348	6.94	11.580	11.493	11.494	11.205
349	6.96	11.582	11.496	11.497	11.210
350	6.98	11.585	11.499	11.499	11.216
351	7.00	11.588	11.502	11.502	11.221